Microinjection of Strong Calcium Buffers Suppresses the Peak of Calcium Release during Depolarization in Frog Skeletal Muscle Fibers

LÁSZLÓ CSERNOCH, VINCENT JACQUEMOND, and MARTIN F. SCHNEIDER

From the Department of Biological Chemistry, University of Maryland, School of Medicine, Baltimore, Maryland 21201

ABSTRACT The effects of high intracellular concentrations of various calcium buffers on the myoplasmic calcium transient and on the rate of release of calcium (R_{rel}) from the sarcoplasmic reticulum (SR) were studied in voltage-clamped frog skeletal muscle fibers. The changes in intracellular calcium concentration ($\Delta[Ca^{2+}]$) for 200-ms pulses to 0–20 mV were recorded before and after the injection of the calcium buffer and the underlying R_{rel} was calculated. If the buffer concentration after the injection was high, the initial rate of rise of the calcium transient was slower after injection than before and was followed by a slow increase of $[Ca^{2+}]$ that resembled a ramp. The increase in myoplasmic $[Mg^{2+}]$ that accompanies the calcium transient in control was suppressed after the injection and a slight decrease was observed instead. After the injection the buffer concentration in the voltage-clamped segment of the fiber decreased as the buffer diffused away toward the open ends. The calculated apparent diffusion coefficient for fura-2 ($D_{app} = 0.40 \pm 0.03 \times 10^{-6}$ cm^2/s, mean ± SEM, $n = 6$) suggests that ~65–70% of the indicator was bound to relatively immobile intracellular constituents. As the concentration of the injected buffer decreased, the above effects were reversed. The changes in $\Delta[Ca^{2+}]$ were underlined by characteristic modification of R_{rel}. The early peak component was suppressed or completely eliminated; thus, R_{rel} rose monotonically to a maintained steady level if corrected for depletion. If R_{rel} was expressed as percentage of SR calcium content, the steady level after injection did not differ significantly from that before. Control injections of anisidine, to the concentration that eliminated the peak of R_{rel} when high affinity buffers were used, had only a minor effect on R_{rel} , the peak was suppressed by 26 ± 5% (mean ± SE, n = 6), and the steady level remained unchanged. Thus, the peak component of R_{rel} is dependent on a rise

Address reprint requests to Dr. Martin F. Schneider, Department of Biological Chemistry, University of Maryland, School of Medicine, Baltimore, MD 21201.

Dr. Csernoch's present address is University Medical School of Debrecen, Department of Physiology, Debrecen, P.O. Box 22, 4012, Hungary. Dr. Jacquemond's present address is Université de Tours, Faculté des Sciences et Techniques, Laboratoire d'Electrophysiologie et de Pharmacologie Cellulaires, Parc de Grandmont, 37200 Tours, France.

J. GEN. PHYSIOL. © The Rockefeller University Press · 0022-1295/93/02/0297/37 $2.00
Volume 101 February 1993 297–333

in myoplasmic [Ca^{2+}], consistent with calcium-induced calcium release, whereas the steady component of R_{rel} is independent of myoplasmic [Ca^{2+}].

INTRODUCTION

Ideas as to how calcium release from the sarcoplasmic reticulum (SR) in skeletal muscle is controlled have undergone major changes in the last two decades. In the late 1960s two groups (Endo, Tanaka, and Ogawa, 1970; Ford and Podolsky, 1970) showed that raising the [Ca^{2+}] in the solution bathing skinned skeletal muscle fibers results in the release of calcium from the SR (calcium-induced calcium release). Since lowering external calcium reduces twitches and K^+ contractures (Frank, 1958; Lüttgau, 1963), calcium ions entering through voltage-gated calcium channels were thought to induce the opening of the SR calcium release channels. Though this mechanism seems to be operating in cardiac cells (London and Krueger, 1986; Beuckelmann and Wier, 1988), data have accumulated that rule out extracellular calcium as the key step in skeletal muscle excitation–contraction (E-C) coupling. It has been shown (Armstrong, Bezanilla, and Horowicz, 1972; Lüttgau and Spiecker, 1979) that skeletal muscle continues to twitch in a nominally calcium-free external milieu. The time course of K^+ contractures was not modified significantly when Ni^{2+}, a nonpermeant cation, replaced Ca^{2+} in the extracellular solution (Caputo, 1972). Furthermore, the calcium release is a monotonically increasing function of membrane voltage, whereas the calcium current, i.e., the amount of calcium entering through voltage-gated channels, decreases at positive potentials as the depolarization approaches the calcium equilibrium potential (Brum, Stefani, and Ríos, 1987). These authors concluded that extracellular calcium entry plays no role in triggering SR calcium release.

The discovery (Schneider and Chandler, 1973) and detailed characterization of intramembranous charge movement (for review, see Ríos and Pizarro, 1991) led to the suggestion that the voltage-sensitive step in E-C coupling is the conformational change of a charged molecule, presumably the dihydropyridine (DHP) receptor (Ríos and Brum, 1987; Tanabe, Takeshima, Mikami, Matsuo, Hirose, and Numa, 1987). Though several mechanisms have been suggested by which the movement of the voltage sensor might be coupled to the opening of the SR channels (Ríos, Pizarro, and Stefani, 1992*b*), the original "mechanical plunger" proposition of Chandler, Rakowski, and Schneider (1976) has gained new attention due to the work of Ríos, Karhanek, González, and Ma (1992*a*).

In the meantime, further evidence has accumulated on the calcium sensitivity of the SR release channel. Calcium-induced release of calcium has been demonstrated in SR vesicles (Meissner, Darling, and Eveleth, 1986) and subcellular bundles of myofibrils (Fabiato, 1984). The isolated release channel, the ryanodine receptor (Fleischer, Ogunbunmi, Dixon, and Fleer, 1985; Imagawa, Smith, Coronado, and Campbell, 1987), was shown to have a profound increase in open channel probability when the extraluminal calcium was raised (Smith, Coronado, and Meissner, 1986).

Using the unique stoichiometry of the DHP and ryanodine receptors, where only every other ryanodine receptor may face a DHP receptor cluster (Block, Imagawa, Campbell, and Franzini-Armstrong, 1988), Ríos and Pizarro (1988) suggested a dual control of SR calcium release. Those release channels that are in direct opposition to

a DHP receptor would be under voltage sensor control (i.e., the mechanical plunger hypothesis), whereas the others would be opened by calcium. In this model the trigger calcium comes from the SR itself, through channels opened by the voltage sensor. Jacquemond, Csernoch, Klein, and Schneider (1991*a*) have provided experimental evidence in favor of this dual control by demonstrating that intracellular injections of ~4 mM BAPTA (1,2-*bis*-[*o*-aminophenoxy]ethane-*N,N,N',N'*-tetraacetic acid), a high affinity calcium buffer, eliminated the calcium transient and selectively suppressed the early peak component of R_{rel}. The selective suppression of the peak R_{rel} by low concentrations of tetracaine (Pizarro, Csernoch, Uribe, and Ríos, 1992), a drug that also blocks calcium-induced calcium release (Endo, 1985) and reduces the open channel probability of the ryanodine receptor (Xu, Jones, and Meissner, 1990), further strengthened the above hypothesis.

On the other hand, Baylor and Hollingworth (1988) and Hollingworth, Harkins, Kurebayashi, Konishi, and Baylor (1992) found that the injection of fura-2 into intact fibers increased the calcium released during an action potential. The only difference between the above measurements and those of Jacquemond et al. (1991*a*) was the preparation (i.e., intact fibers in the above vs. voltage-clamped cut fibers in Jacquemond et al. [1991*a*]) and the fact that the intracellular $[Ca^{2+}]$ increase was not completely suppressed in the above but was in Jacquemond et al. (1991*a*).

In this study we extended the measurements of Jacquemond et al. (1991*a*) by examining different affinity buffers. These results are consistent with the idea that the initially released calcium opens further release channels and participates in a calcium-induced calcium release mechanism.

Part of this work has been presented in abstract form (Csernoch, Jacquemond, Kao, and Schneider, 1992).

METHODS

Experimental

Single skeletal muscle fibers of the frog, *Rana pipiens*, were dissected from the semitendinosus muscle in Ringer's solution, cut in relaxing solution, and mounted into a double Vaseline-gap chamber (Kovács, Ríos, and Schneider, 1983). Fibers were stretched beyond filament overlap (sarcomere length > 3.8 μm) to avoid movement. After completing the Vaseline isolation, the relaxing solution was exchanged in the middle pool to external solution containing (mM) 125 $TEACH_3SO_3$, 2 $CaCl_2$, 5 Cs-HEPES (*N*-2-hydroxyethylpiperazine-*N'*-2-ethanesulfonic acid) buffer, and 10^{-7} g/ml tetrodotoxin, and in the open end pools to internal solution containing (mM) 102.5 Cs glutamate, 5.5 $MgCl_2$, 5 ATP, 4.5 Na-Tris-maleate buffer, 13.2 Cs-Tris-maleate buffer, 0.1 EGTA, 5 creatine phosphate, 6 glucose, 1 APIII, and 0.05 fura-2. In a few fibers K glutamate was used instead of Cs glutamate in the internal solution. Calcium transients, calcium release, and the effects of injected calcium buffers were essentially the same with Cs^+ or K^+ as predominant internal cation.

The fibers were trans-illuminated using a tungsten halogen light source and a long pass filter (cut on wavelength = 550 nm) for absorbance and epi-illuminated (at 358 or 380 nm) using a xenon arc lamp for simultaneous fluorescence measurements (Klein, Simon, Szücs, and Schneider, 1988). The intact middle segment of the fibers was voltage clamped to −100 or −90 mV. From this holding potential (V_h), depolarizing pulses were applied and the accompanying changes in membrane current, voltage, and transmitted and fluorescent light intensities were

recorded. Appropriate dichroic mirrors were used to dissect the changes in light intensity at 510 nm, due to fura-2 fluorescence, and at 590, 700, and 850 nm, due to changes in APIII and intrinsic fiber absorbance. Detailed descriptions of the experimental apparatus and the recording of the data are given elsewhere (Klein et al., 1988; Jacquemond and Schneider, 1992). All measurements were carried out at 8–10°C.

Microinjection

The optical setup was modified in order to enable continuous observation of the fiber during the injection. The fiber was illuminated at 590 nm and the transmitted light image was projected onto an image intensifier (KS-1381; Video Scope International Ltd., Washington, DC) using lenses and a full mirror in place of one of the dichroic mirrors. The image intensifier was coupled to a commercial video camera and monitor giving a real-time image of the fiber with an approximate magnification of either 500 or 1,000. For 1 in every 5 s the fiber was also epi-illuminated with 358 nm for the detection of fura-2 fluorescence.

Calcium buffers were microinjected into the fibers from a glass microelectrode after impalement. The resistance of the electrodes used ranged between 50 and 100 MΩ when filled with the injected solution, or between 3 and 6 MΩ when filled with 3 M KCl. If the impalement was considered successful (see below), the pressure in the electrode was increased slowly to 4–8 psi using a Picospritzer II (General Valve Corp., Fairfield, NJ). In most cases this was sufficient to start the injection, which was kept going until the desired concentration was reached (see below for a discussion of how the concentration of the injected buffer was calculated). In some fibers higher initial pressure values were needed to start the injection than to keep it continuously going, which we attributed to clogging of the electrode during penetration since the electrodes were always functional if removed from the fiber. Though fibers usually tolerated successive impalements, results from multiple impalements are not included in this study.

Injected Solutions

Four different calcium buffers were used in these experiments, all structurally related to fura-2, namely, BAPTA, Br_2BAPTA (5,5′-dibromo-BAPTA), F_2BAPTA (4,4′-difluoro-BAPTA), and fura-2 itself. As a control, anisidine (anisidine-*N,N′*-diacetic acid, structurally "half-BAPTA") was used. The injection pipette contained (mM) 10–50 of either of the above buffers, or anisidine, in their potassium salt form; 0.5 fura-2, as tracer in the non-fura-2 injections; 1–5 HEPES (ratio of buffer to HEPES was always 10:1); and $CaCl_2$ to set the nominal free calcium to ~50 nM as calculated using the dissociation constant given by Molecular Probes, Inc. (Eugene, OR; Haugland, 1989) for each buffer.

Fura-2, BAPTA, Br_2BAPTA, and F_2BAPTA were purchased from Molecular Probes, Inc., APIII was from ICN Biochemicals, Inc. (Cleveland, OH), and anisidine-*N,N′*-diacetic acid was a generous gift from Dr. J. P. Y. Kao, who synthesized the compound. All other reagents were of analytical grade.

Criteria for Successful Injection

An injection was considered successful if no visible damage could be seen on the fiber and if the holding current did not increase after the removal of the microelectrode. In ~10% of the cases one, or usually both, of the above criteria was not satisfied, and those fibers were not analyzed further. Furthermore, in another 10% of the cases the microelectrode clogged during the impalement (see above), and though fibers were usually reimpaled and injected, these injections are also not included in the analysis.

When pressure values of 10 psi or above were needed to start the injection, local "swelling" was sometimes observed ("balloon injection"), which dissipated with time in a few seconds since the pressure was immediately decreased. Though local damage could not be ruled out, the

overall effect was considered negligible on the basis that control fibers reaching a 15% increase in diameter at the site of injection showed little change in calculated R_{rel} (an example is shown in Fig. 6).

"Strong," "Medium," and "Weak" Injections

As judged by the effects on the kinetics of the APIII calcium transients, the injections could be separated into one of three classes. If the amount of buffer was sufficient to completely abolish the APIII signal, the injection is referred to as a strong injection. This occurred when several millimolar of high affinity buffer was injected. In some cases, as will be shown in a future publication (Csernoch, L., V. Jacquemond, and M. F. Schneider, manuscript in preparation), the APIII calcium transient was not completely suppressed, but its kinetics were dramatically altered by the injection: it had a small and fast initial rising phase, a plateau, and a secondary rising phase. These injections will be referred to as medium injections. They were seen with high affinity buffer concentrations up to ~1 mM. All other injections, including all anisidine injections regardless of the amount injected, produced only minor changes in the APIII calcium transient and will be termed weak. The above terminology is based on the APIII calcium transient measured during the first pulse after injection, which was to 0 mV or to a more positive potential to insure near-maximal fiber activation. Later in the course of an experiment, after a strong injection, the APIII calcium transients often acquired the characteristics of medium injections, as expected from the decreased buffer concentration due to diffusion of buffer away from the injection site.

Determination of Fura-2 and Injected Buffer Concentration

The total concentration of fura-2 ($[\text{fura-2}]_T$) was calculated from the fluorescence (F) measured with an excitation wavelength of 358 nm (F_{358}) after correcting for APIII absorbance as described earlier (Klein et al., 1988). To calculate the total concentration of the injected buffer ($[B]_T$), we coinjected fura-2 and assumed that the ratio of injected buffer to injected fura-2 was equal to that in the pipette. That is, $[B]_T$ equals the increase in fura-2 concentration multiplied by the ratio of buffer concentration over fura-2 concentration in the pipette.

Calculation of the Changes in Free $[Ca^{2+}]$ and $[Mg^{2+}]$

Changes in free $[Ca^{2+}]$ were calculated from the changes in APIII absorbance (APIII calcium transient), measured at 700 nm, after correcting for changes in the intrinsic absorbance, measured at 850 nm, as described earlier (Kovács et al., 1983; Klein et al., 1988). After the microinjection of high affinity calcium buffers to millimolar concentrations, the change in free $[Ca^{2+}]$ was usually too small to be detected by the relatively low affinity calcium indicator APIII. In this case the fura-2 fluorescence was used to calculate the changes in $[Ca^{2+}]$ (fura-2 calcium transient) as described in the following section.

The absorbance changes at the isosbestic wavelength of APIII for calcium (590 nm) were used to determine the changes in free $[Mg^{2+}]$ as described earlier (Irving, Maylie, Sizto, and Chandler, 1989; Jacquemond, Klein, and Schneider, 1990; Jacquemond and Schneider, 1992).

Calculation of the Calcium Bound to Fura-2

To calculate the relative saturation, y_f, of fura-2 with calcium ($y_f = [\text{Ca-fura-2}]/[\text{fura-2}]_T$, where [Ca-fura-2] denotes the concentration of calcium bound to fura-2), the fluorescence intensities, as excited at 380 and 358 nm (F_{380} and F_{358}, respectively), were first determined. F_{358} was calculated for each pulse from bracketing measurements in time using linear interpolation (Klein et al., 1988). The 358-nm filter was set to be the isosbestic wavelength for calcium (Klein et al., 1988), which was rechecked after every few experiments, and the interference filter was tilted or changed if necessary, since we found that the filter tended to shift slightly to shorter

center wavelengths over time. With 358 nm as the isosbestic wavelength, the relative saturation becomes

$$y_f = (R - R_{min})/(R_{max} - R_{min}) \quad (1)$$

where R denotes the fluorescence ratio F_{380}/F_{358} and R_{min} and R_{max} denote the values of R when no calcium is bound to fura-2 and when fura-2 is fully saturated with calcium, respectively. R_{max} was obtained together with the $k_{on,f}$ and $k_{off,f}$ (forward and backward rate constants of the fura-2–calcium binding reaction, respectively) by fitting the differential equation

$$dR/dt = k_{on,f}\cdot[Ca^{2+}]\cdot(R_{max} - R) - k_{off,f}\cdot(R - R_{min}) \quad (2)$$

using the free $[Ca^{2+}]$ calculated from the APIII absorbance in each fiber as described in detail by Klein et al. (1988). R_{min} was determined in separate fibers using 5 mM EGTA and no added calcium in the internal solution.

In the case of strong injections, the absorbance change from APIII was too small to allow the determination of the free $[Ca^{2+}]$, and hence the above analysis of the fura-2 parameters could not be carried out. Instead, the parameters (R_{max}, $k_{on,f}$, and $k_{off,f}$) determined before injection were used. Furthermore, rearranging Eq. 2 and solving for $[Ca^{2+}]$ allowed us to calculate the free $[Ca^{2+}]$ in the presence of high buffer concentrations.

Time Course of Calcium Bound to Injected Buffers

The calcium bound to any injected buffer ([Ca-B]) was calculated from numerical integration of the first-order binding reaction

$$dy_B/dt = k_{on,B}\cdot[Ca^{2+}]\cdot(1 - y_B) - k_{off,B}\cdot y_B \quad (3)$$

where $y_B = [Ca\text{-}B]/[B]_T$, while $k_{on,B}$ and $k_{off,B}$ denote the forward and backward rate constants of the calcium–buffer reaction, respectively. Using the value of $k_{on,f}$ for $k_{on,B}$, the value of $k_{off,B}$ for the buffers Br_2BAPTA and F_2BAPTA was set so that the resulting $K_{d,B}$ ($=k_{off,B}/k_{on,B}$, dissociation constant of the buffer) would equal that given by Molecular Probes, Inc. (Haugland, 1989; 1.58 and 2.45 μM, respectively). For fura-2 and BAPTA, both $k_{on,B}$ and $k_{off,B}$ were set equal to the corresponding value of fura-2.

In strong injections, that is, when the fura-2 calcium transients were used, the above calculation resulted in a time course of [Ca-B] identical to that of the fluorescence change in the case of fura-2 and BAPTA, whereas in the case of Br_2- and F_2BAPTA the time course of [Ca-B] was different from that of [Ca-fura-2] due to their higher values of $k_{off,B}$.

In the case of all medium and weak injections, since the free $[Ca^{2+}]$ increase was not suppressed and hence fura-2 was saturated during much of the pulse, the APIII calcium transient was used in Eq. 3 with $k_{on,B}$ and $k_{off,B}$ determined as described above. For anisidine, a $K_{d,B}$ of 1 mM was used.

Calculation of R_{rel}

The general procedure for calculating R_{rel} from the APIII calcium transient before injection followed the line described by Melzer, Ríos, and Schneider (1987) and Klein, Simon, and Schneider (1990). In our calculations, the calcium binding of three myoplasmic binding sites (namely, troponin C, parvalbumin, and the SR calcium pump), two dyes (APIII and fura-2), and the injected buffer were considered together with the transport of calcium into the SR via the calcium pump.

The calcium binding to fura-2 and to the injected buffer was calculated as described above. To calculate the calcium binding to the other sites, troponin C, parvalbumin, pump, and APIII (termed "noninjected sites" hereafter), their calcium binding properties ("removal

parameters") were either assigned or determined from fits to the falling phase of several calcium transients before microinjection. The fit to each calcium transient started shortly after repolarization, when R_{rel} is assumed to be zero (Melzer et al., 1987). Usually three of the removal parameters, the maximal pump rate (PV_{max}), $k_{off,\ Mg\text{-}parvalbumin}$, and [parvalbumin], were determined from the fit, whereas the others were taken from biochemical measurements and held constant during the fitting procedure (Klein et al., 1990).

The rate of release of calcium from the SR (R_{rel}) was then calculated from

$$R_{rel} = d([Ca^{2+}] + \Sigma_i[Ca\text{-}S_i] + [Ca\text{-}fura\text{-}2] + P)/dt \quad (4)$$

where $\Sigma_i[Ca\text{-}S_i]$ denotes the calcium bound to the noninjected sites (i = 1–4) and P denotes the calcium transported back into the SR via the calcium pump. After the injection an additional binding site, the injected buffer, sometimes appears in the myoplasm and its calcium binding ([Ca-B]) must be considered also; hence, Eq. 4 modifies to:

$$R_{rel} = d([Ca^{2+}] + \Sigma_i[Ca\text{-}S_i] + [Ca\text{-}fura\text{-}2] + P + [Ca\text{-}B])/dt \quad (4a)$$

In weak injections, as shown in Fig. 6, it was found that the removal parameters determined before injection described the falling phase of the calcium transient after the injection; thus, $d(\Sigma_i[Ca\text{-}S_i])/dt$ and dP/dt were calculated using the same parameters before and after the injection. This, however, was not always the case with strong injections, where the usual removal parameters determined before injection plus the additional injected buffer sometimes failed to describe the falling phase of the fura-2 calcium transient. A detailed description and discussion of this discrepancy are given in Results.

Protocol for a Typical Experiment

The main objective of the experiments presented in this paper was to determine the effects of strong buffering of myoplasmic $[Ca^{2+}]$ on the rate of release of calcium from the SR during sufficiently large depolarizations for maximal activation of release. Pressure microinjection, which was used to introduce calcium buffers into the myoplasm, required not only insertion of the microelectrode and control of the pressure, but also repositioning of sliders in the optical apparatus to change magnification and to direct the image to the image intensifier/video camera port rather than to the beam splitters and photodiode ports during injection. Because these changes had to be made before injection and reversed after injection, and in order to begin recording of optical signals before appreciable diffusion of buffers away from the injection site (i.e., as soon as possible after the microinjection), we elected to use a protocol that minimized other experimental manipulations.

The basic protocol that we adopted was to first monitor optical and electrical signals for depolarizing pulses of several amplitudes and durations before microinjection to provide control measurements to characterize the calcium removal properties of the uninjected fiber. A 200-ms pulse to 20 mV was then applied to characterize the control calcium release for a maximal activation before injection. The optical components were then changed, the injection was carried out, the components were rapidly changed back, and the 200-ms pulse to 20 mV was repeated as soon as possible after injection to determine release during maximal activation when the buffer effect was the strongest. In most experiments pulses for monitoring charge movement were not applied in order to avoid further complication of an already rather involved experimental protocol. Since the final decay of $[Ca^{2+}]$ after pulses following buffer injection was quite slow, 1–2 min were generally allowed for recovery between pulse applications. Although many fibers survived for long periods after strong (or weak) injections and exhibited recovery of calcium transients as the injected buffer diffused away to the cut ends of the fiber, this article concentrates on results obtained shortly before and shortly after injection.

Statistical significance was calculated with a Student's paired t test.

RESULTS

Diffusion Properties of the Injected Fura-2

After the injection was completed and the pipette removed from the fiber, the concentration of the injected buffer monotonically decreased due to its diffusion toward the open ends. Fig. 1 shows the concentration of fura-2 during the course of

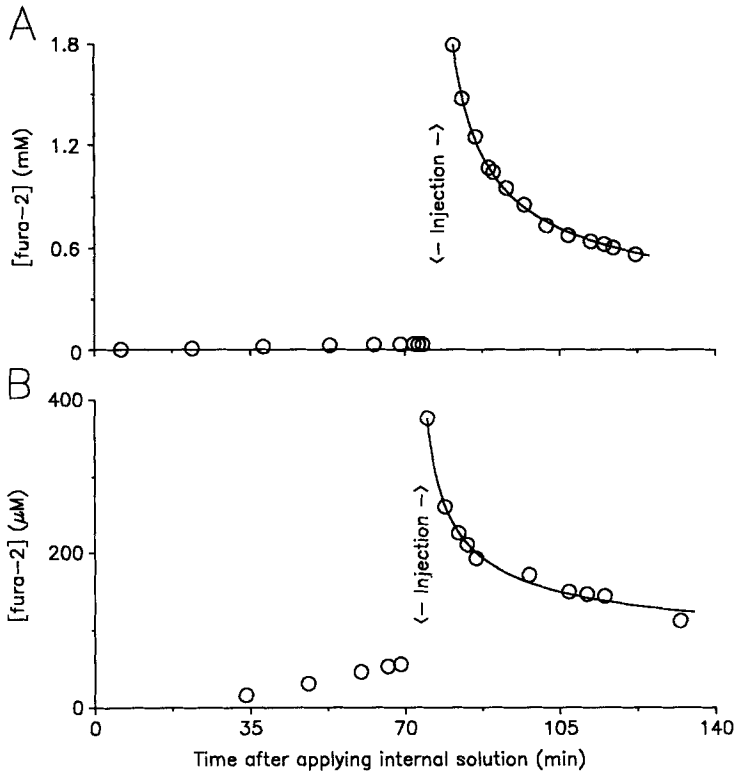

FIGURE 1. Time course of fura-2 concentration in injection experiments in two different fibers. The injection pipette contained 10 mM fura-2 as the sole buffer in *A* and 10 mM BAPTA with 0.5 mM fura-2 in *B*. Note that the vertical scale is different for the two panels. The points after injection were fitted assuming linear diffusion (Eq. 5), resulting in an apparent diffusion coefficient of 0.42×10^{-6} cm^2/s for both fibers. The time of injection, the other fitted parameter in Eq. 5, was 76.7 and 72.2 min for *A* and *B*, respectively. Fibers 851 and 803, path length (pl) 88 and 70 μm, V_h −90 and −100 mV.

two injection experiments. In the first fiber (Fig. 1 *A*) fura-2 was injected alone as the calcium buffer, in this case to a final concentration of 2.1 mM, whereas in the case of the fiber in Fig. 1 *B* fura-2 was coinjected with BAPTA so the final concentration of fura-2 was only 381 μM. Before injection fura-2 was diffusing from the open ends and reached concentrations of 28.3 and 56.6 μM for the fibers in Fig. 1, *A* and *B*, respectively.

Assuming linear diffusion and that the measurements were made at the site of injection, the data points after injection were fitted with:

$$C(t) = C_b + M/[4 \cdot \pi \cdot D_{app} \cdot (t - t_0)]^{1/2} \quad (5)$$

where $C(t)$ denotes the concentration of fura-2 at time t, C_b the concentration before injection, M the total amount injected at t_0, and D_{app} the apparent diffusion coefficient (Crank, 1975). In general M should be calculated as

$$M = \int C(x, t = t_0)\, dx \quad (6)$$

where $C(x, t = t_0)$ is the concentration at distance x, and the integration goes from minus infinity to plus infinity. Since in our case the detection only sees the portion of the fiber that has been illuminated, a circular spot with a diameter of 300 μm, and since no spatial information is available from within that spot, Eq. 6 simply reduces to

$$M = l_{spot} \cdot C(t = t_0) \quad (6a)$$

where l_{spot} is the length of the fiber illuminated.

Fig. 1 shows the least-squares fit of Eq. 5 to the data points after injection with t_0 and D_{app} as the free parameters. For both fibers the calculated apparent diffusion coefficient for fura-2 was 0.42×10^{-6} cm^2/s, in good agreement with earlier results (Konishi, Olson, Hollingworth, and Baylor, 1988). From six fibers, where at least 40 min of recording was available after injection, the average D_{app} was $0.40 \pm 0.03 \times 10^{-6}$ cm^2/s (mean ± SEM). These results further strengthen the idea of intracellular binding of fura-2 (Baylor and Hollingworth, 1988) and demonstrate that the binding sites were not lost due to the cutting of the fiber, as expected if the sites were relatively immobile. It is also worth noting that the relative binding seems to be independent of the fura-2 concentration (at least in the range of 200 μM– 2 mM), suggesting that the binding site is far from saturation.

Suppression of $\Delta[Ca^{2+}]$ Due to a Strong Injection

Changes in the concentration of free calcium, free magnesium, and calcium bound to fura-2 recorded just before and just after the injection of 5.8 mM BAPTA are presented in Fig. 2. Before injection, a depolarizing pulse to +20 mV for 200 ms elicited a relatively large calcium transient (Fig. 2 *A, left*), with a peak value of 5.9 μM, that saturated the fura-2 early in the pulse (Fig. 2 *B, left*). There was a slow increase in the free $[Mg^{2+}]$ throughout the calcium transient (Fig. 2 *C, left*), as previously observed (Irving et al., 1989; Jacquemond et al., 1990), as the Mg^{2+} dissociated from the high calcium affinity sites of parvalbumin and troponin C in exchange for calcium.

The normal increase in $[Ca^{2+}]$ was almost completely eliminated after the injection of the buffer (Fig. 2 *A, right*), as reported earlier (Jacquemond et al., 1991*a*). Furthermore, the increase in free $[Mg^{2+}]$ was also abolished, consistent with the absence of any sizable calcium transient, and it actually showed a slight decrease after the stimulus (Fig. 2 *C, right*). This could reflect the movement of Mg^{2+} from the myoplasm into the SR in exchange for some of the released calcium (Jacquemond et al., 1991*b*).

The fura-2 saturation, nevertheless, increased during the pulse (Fig. 2 *B, right*),

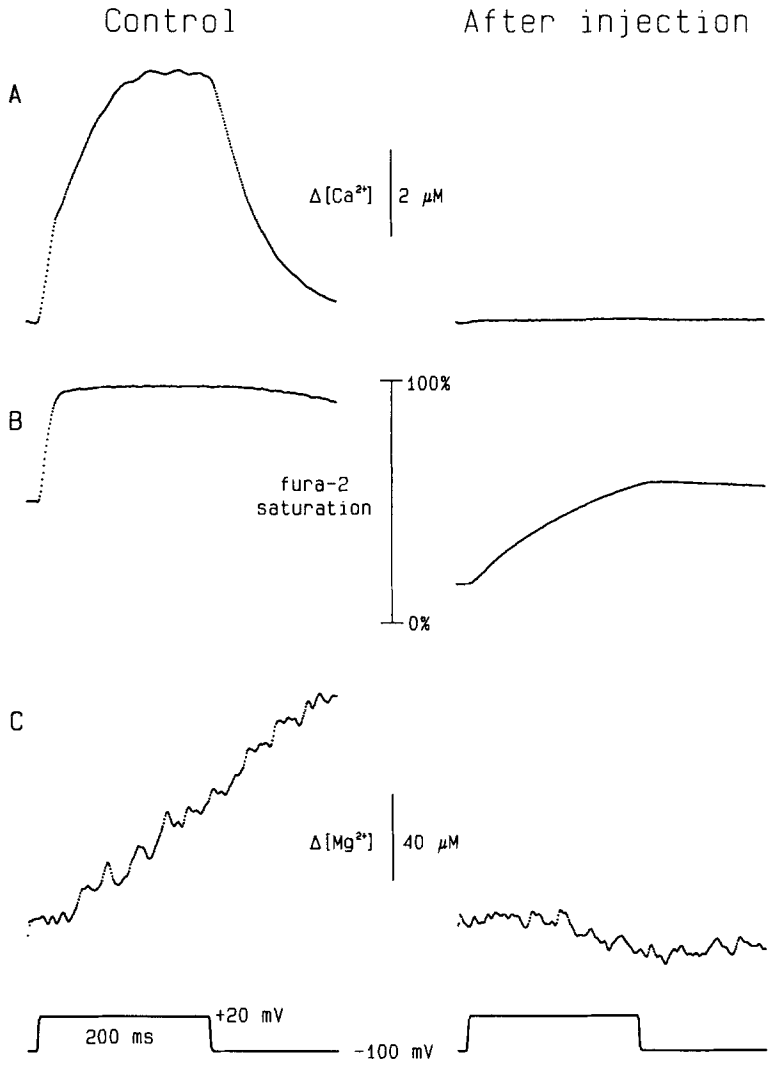

FIGURE 2. Changes in intracellular free $[Ca^{2+}]$ (*A*) and $[Mg^{2+}]$ (*C*) and the relative saturation of fura-2 with calcium (*B*) right before (*Control*) and after the injection of 5.8 mM BAPTA. Before injection the depolarizing pulse (protocol shown on lowermost traces) brought about a 5.8 μM increase in $[Ca^{2+}]$ (*A*) that resulted in an early saturation of fura-2 (*B*) and an increase in $[Mg^{2+}]$ (*C*) due to an exchange of calcium for magnesium on parvalbumin and troponin C. The injection completely eliminated the calcium (*A*) and, consequently, the magnesium (*C*) transient during the depolarizing pulse; nevertheless, there was a substantial increase in fura-2 saturation (*B*), indicating that calcium was released from the SR but mostly taken up by the injected buffers, i.e., BAPTA and fura-2. Same fiber as in Fig. 1 *B*. Parameters for calculating the fura-2 saturation were $k_{on,f} = 1.12 \times 10^8\ M^{-1}s^{-1}$, $k_{off,f} = 6.5\ s^{-1}$, $R_{max} = 0.28$, and $R_{min} = 1.65$. The resting $[Ca^{2+}]$ was 59 and 11 nM before and after injection, respectively.

indicating that calcium was indeed released from the SR, but essentially all of the released calcium was taken up by the injected fast buffers. Using the procedure described in Methods, the calcium transient after injection was calculated from the fura-2 saturation and revealed an 88-nM increase in $[Ca^{2+}]$ by the end of the 200-ms depolarization (see also Fig. 4 *A, right*). The kinetic parameters used to calculate the fura-2 calcium transient (Eq. 2) in Fig. 2 were $k_{on,f} = 1.12 \times 10^8\ M^{-1}s^{-1}$ and $k_{off,f} = 6.5\ s^{-1}$. These parameters varied slightly from fiber to fiber with average values of $k_{on,f} = 1.19 \pm 0.06 \times 10^8\ M^{-1}s^{-1}$ and $k_{off,f} = 13.4 \pm 0.6\ s^{-1}$ (mean ± SEM, $n = 41$).

The resting saturation of fura-2 decreased after the injection in the fiber shown in Fig. 2, which can be seen as a decrease of the baseline of the traces in Fig. 2 *B*. The corresponding values of resting $[Ca^{2+}]$ were 59 and 11 nM before and after the injection, respectively. As an average of 41 injections, the resting calcium decreased from 84.5 ± 5.8 to 72.6 ± 14.3 nM (mean ± SEM) due to the injection, although in same cases (30% of the total) we observed an increase in resting $[Ca^{2+}]$.

Recovery after Injection

After the injection the concentration of fura-2 (see Fig. 1 *B*), and presumably the concentration of BAPTA as well, decreased at the site of injection as they diffused toward the open end pools. While the concentration of fura-2 was 347 μM 2 min after injection, it decreased to 169 μM after 25 min. Assuming that BAPTA diffused as fura-2 did, this decrease would correspond to a change in BAPTA concentration from 5.8 to 2.2 mM. Had the effects described in the previous section been due to the presence of the high affinity buffers, they should have been partially reversed and the fiber should have recovered to some extent with the decrease in buffer concentration. Fig. 3, *A* and *B* show that this was indeed observed.

The calcium concentration increase during the depolarizing pulse before injection (Fig. 3 *A*, control), which was completely eliminated shortly after the injection (2 min), became detectable by APIII during a pulse applied 25 min after injection, at which time $\Delta[Ca^{2+}]$ reached a maximum of 1.5 μM by the end of the stimulus. The APIII calcium transient 25 min after injection was, nevertheless, still different from that before injection. It exhibited a long initial slow phase of increase in $[Ca^{2+}]$ followed by a faster increase near the end of the pulse.

The reappearance of a detectable APIII calcium transient was accompanied by characteristic changes in the measured fura-2 saturation (Fig. 3 *B*). Shortly after injection (2 and 3 min) the rate of change of fura-2 saturation was relatively slow, only a slight decrease in the rate of change of saturation was observed during the pulse, and fura-2 was far from saturation. In contrast, the fura-2 saturation record measured 25 min after injection increased more rapidly, showed a pronounced decrease in rate of change, and approached full saturation (91%) by the end of the pulse. Since there was good temporal correlation between the close approach to full saturation of fura-2 during the stimulus and the onset of the faster increase in $\Delta[Ca^{2+}]$ as detected by APIII (Fig. 3, 25-min recovery and records from other similar experiments not shown), we believe that the latter was in fact the consequence of the inability of BAPTA and fura-2 to continue to buffer the calcium concentration to nanomolar levels due to their near saturation by calcium.

Similar recovery was observed in each and every fiber, though the extent was different and depended on the concentration of injected buffer shortly after injection. In fibers where the APIII calcium transient was completely suppressed after the injection, as in the fiber in Fig. 3, fura-2 never returned to its preinjection level and full recovery was never observed. On the other hand, in the case of small injections,

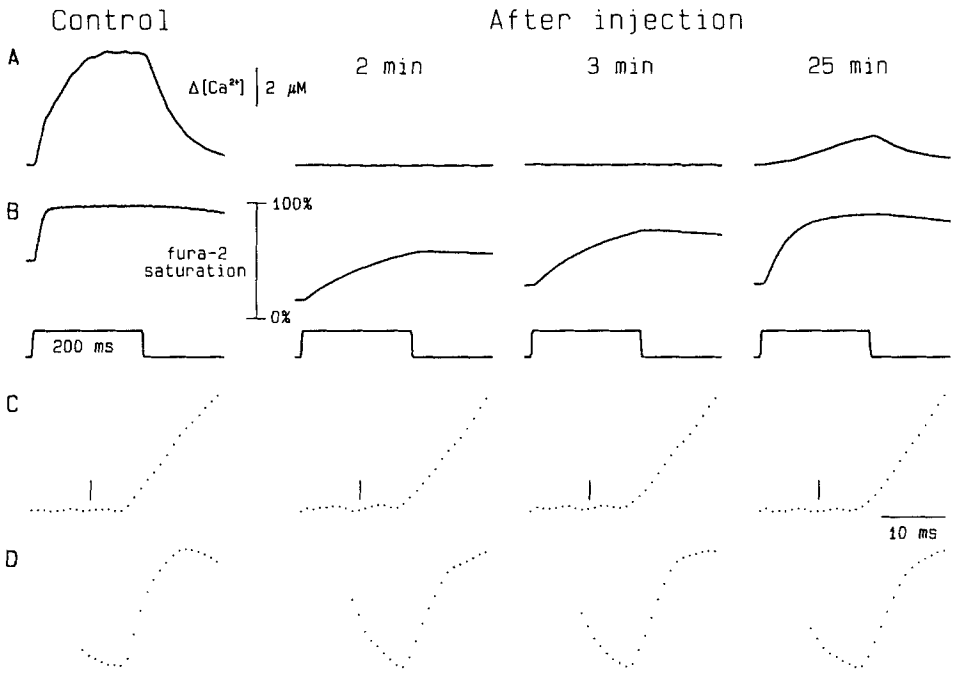

FIGURE 3. Recovery of the APIII calcium transient (*A*) and the fura-2 saturation (*B*) after the injection. The transients were recorded right before (*Control*) and 2, 3, and 25 min after the injection when the concentration of fura-2 was 56.6 and 347, 318, and 169 μM, respectively. If the diffusion of BAPTA was identical to that of fura-2, the corresponding BAPTA concentrations after the injections were 5.8, 5.2, and 2.2 mM. (*C*) Changes in the latency of the fura-2 saturation. The points from the first 30 ms of the transients in *B* were scaled so the first and last points would be equal after scaling and also expanded in time to show every individual data point. Vertical lines above each record mark the onset of the pulse. To calculate the latency for each transient, straight lines were fitted to the records, starting with the first nine points and including more and more points in the fit, and the error of the slope was plotted, on an arbitrary scale, as the function of points included into the fit (*D*). The lowest value of the error marks the last point of the latency period (for further details see text) and was thus calculated to be 5, 7, 6, and 6 ms in control and 2, 3, and 25 min after injection, respectively. Same fiber as in Fig. 2.

the peak of the calcium transient could actually be greater after injection than before (data not shown). Since the diffusion of BAPTA might not be the same as that of fura-2, further aspects of recovery are not discussed in this paper. A more detailed description will be presented elsewhere (Csernoch, L., V. Jacquemond, and M. F. Schneider, manuscript in preparation).

Latency of the Calcium Transients after Injection

Hollingworth et al. (1992) suggested that some of the effects on the calcium transients seen after injection might be due to local damage caused by the injection. In their case this manifested as a slowing down of the processes leading to calcium release. We examined this possibility by calculating the latencies of our transients.

Fig. 3 *C* shows the first 30 ms of each corresponding transient from Fig. 3 *B*, scaled so that the first point and last point of each scaled record have the same values (note that the time scale in *C* has been expanded by ~10 times compared with that in *B*). For each record, 10 points were sampled before the onset of the depolarizing pulse (marked by vertical lines above each record). To calculate the latency, straight lines were fitted to the data points starting from the first point and including an increasing number of points for each consecutive fit. As long as the points fall on a straight line, that is, until the onset of the transient, the error of the slope in the fit decreases (Close, 1981). Fig. 3 *D* plots the error of the slope on an arbitrary scale, starting with the first nine and ending when all 30 points were included in the fit. All four records go through a local minimum which thus marks the last point of the latency period. The calculated latency values were 5, 7, 6, and 6 ms for the records before and 2, 3, and 25 min after injection, respectively. Though the change in latency from before injection to after injection, 2 ms, is comparable to that reported by Hollingworth et al. (1992) for the decrease in time to half-peak of calcium bound to fura-2, 1.6 ms, a similar decrease with time after injection as they observed was not seen in the present experiments.

As an average of 41 injections, the latency increased from 5.2 ± 0.2 ms (mean ± SEM) before injection to 7.4 ± 0.5 ms after injection. There was no significant change in the latency during recovery.

Suppression of R_{rel} after the Injection

To calculate the amount of calcium released from the SR, the calcium bound to various intracellular binding sites has to be determined first. Fig. 4 shows the calcium distribution among these sites before and after injection (left and right columns, respectively). Three pulses of increasing duration to −20 mV (Fig. 4 *A*) were used to determine the removal parameters (see Methods). The predicted decline of the calcium transient after repolarization is shown both for these three traces and for the pulses to +20 mV before and after injection as the noiseless curves. Note that the scale for $\Delta[Ca^{2+}]$ after injection (Fig. 4 *A, right*) is expanded 75 times compared with that before injection (Fig. 4 *A, left*).

Using the removal parameters determined from the fits to the decay of $\Delta[Ca^{2+}]$ after the control pulses to −20 mV, the calcium bound to the noninjected sites was calculated before and after injection (Fig. 4 *C*). It had an initial fast rising phase followed by a slow rising phase in control, of which only the latter was present after injection. Furthermore, as expected from the difference in $\Delta[Ca^{2+}]$, the increase in the amount bound to these sites was ~4.5 times greater (894 vs. 197 μM) before injection than after. In contrast, the increase in the calcium bound to fura-2 and to the injected buffer (Fig. 4 *B*) was negligible before the injection, but became

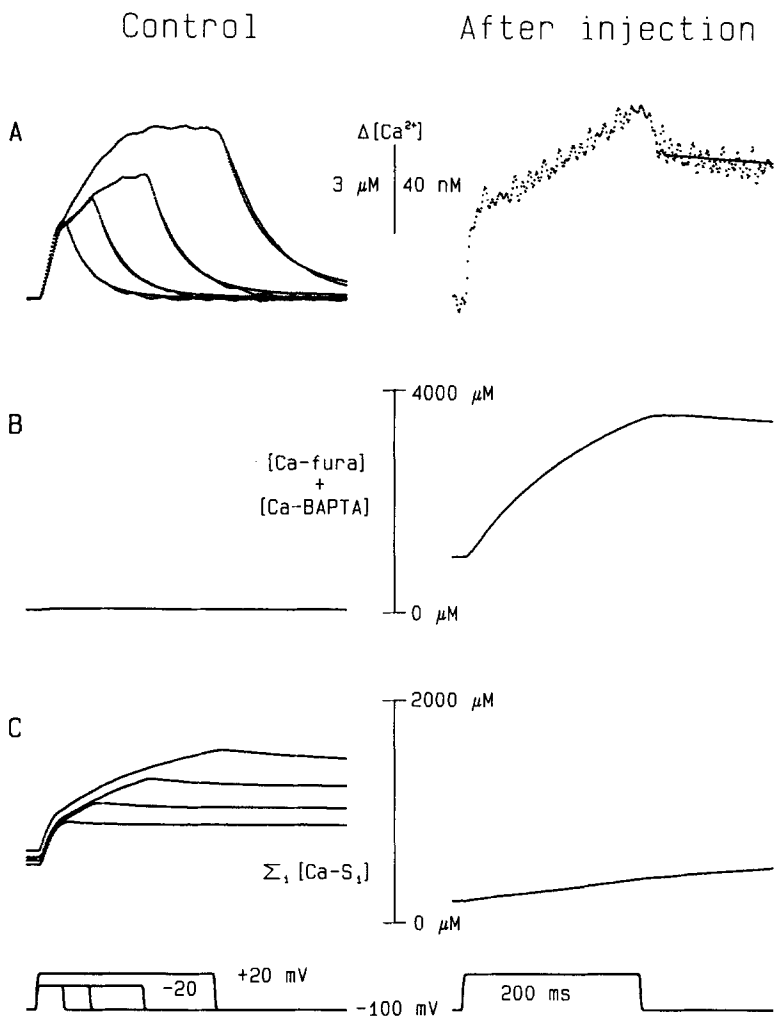

FIGURE 4. The distribution of released calcium among different binding sites before (*Control*) and after the injection of BAPTA (*After injection*). The changes in intracellular free $[Ca^{2+}]$ (*A*) were calculated from APIII absorbance and from fura-2 fluorescence before and after injection, respectively, as described in Methods. Note that the scale for the postinjection record is expanded 75 times compared with that before injection. Three pulses, of 30-, 60-, and 120-ms duration, to −20 mV from before injection were used to determine the removal parameters as described in Methods. The noiseless traces superimposed on each record are the predicted decays of the calcium transients after repolarization as calculated using the parameter values [parvalbumin] = 1,702 μM, $k_{off,Mg\text{-}parvalbumin}$ = 4.07 s^{-1}, PV_{max} = 1,114 μM s^{-1}, and $K_{d,pump}$ = 1 μM with all other parameters the same as those given by Klein et al. (1990). (*B*) The calcium bound to fura-2 and to fura-2 plus BAPTA before and after injection, respectively. The rate constants for the calcium–fura-2 reaction are given in the legend of Fig. 2. (*C*) Calcium bound to the noninjected sites. The parameters to calculate the binding were determined from the above described fits. Note that the vertical scale in *C* was expanded twice compared with that in *B*. The pulse protocol is given at the bottom. Same fiber as in Fig. 2.

dominant (93% of total released calcium) after the injection. Thus the main sink for calcium removal changed from the intrinsic to the injected buffers after the injection.

The total amount of calcium released is the sum of all three rows in Fig. 4 plus the calcium transported back into the SR via the calcium pump (161 and 12 μM before and after injection, respectively, using PV_{max} = 1,114 μM s^{-1}). The simple addition leads to 1.08 and 2.48 mM of calcium released from the SR before and after the injection, respectively. These values were determined predominantly by the calcium bound to the noninjected sites before and by the calcium bound to fura-2 and BAPTA after the injection (above). Had the parameters used to calculate calcium binding to either or both classes of sites been incorrect, the amounts would not be directly comparable. It is worth noting that since the calcium bound to fura-2 relied on parameters directly measured in our system, its error was probably smaller than that of calcium bound to the noninjected sites, the calculation of which depended partially on biochemical data. Alternative parameter values for the noninjected sites will be considered in connection with Fig. 10.

Using the total amount of calcium released, the rate of calcium release from the SR was calculated and is shown in Fig. 5 *A* before (*left*) and after (*right*) injection. Before injection R_{rel} exhibited an early peak followed by a fast decline due to calcium-dependent inactivation of the release channels (Schneider and Simon, 1988) and then a slow decline due to depletion of calcium from the SR (Schneider, Simon, and Szücs, 1987). After the injection the fast decline was absent, leaving only the slowly declining phase. Single exponential plus constant fits to the slow phase, from the 50th ms to the end of the pulse, revealed similar rate constants, 80.9 and 108.0 ms^{-1} before and after the injection, respectively, showing that the mechanism underlying the slow decline was probably the same in both cases.

To correct the R_{rel} records for the effects of depletion of calcium from the SR, the value of the R_{rel} record at each time point t, $R_{rel}(t)$, was multiplied by $C_0/[C_0 - I(t)]$, where C_0 is the calcium content of the SR before the stimulus and $I(t)$ represents the running integral of R_{rel} at time t (Schneider, Simon, and Klein, 1989), to obtain the depletion-corrected record denoted by $R^*_{rel}(t)$. The SR calcium contents used in the calculations for the fiber in Fig. 5 were 1.45 and 3.30 mM before and after the injection, respectively, expressed as the equivalent $[Ca^{2+}]$ if the entire SR content were free $[Ca^{2+}]$ in the myoplasmic water. Since the resting free $[Ca^{2+}]$ decreased due to the injection (see Fig. 2 and related text), this relatively large apparent increase in SR content is most likely explained as being the result of inconsistent relative scaling of the calcium bound to the noninjected and injected buffers. Assuming that the injection itself had no effects on the SR calcium content, R^*_{rel} and R_{rel} were normalized to C_0 (Fig. 5, *B* and *C*) to correct for the error in the relative scaling. Note also that R^*_{rel}/C_0 should be proportional to the number of open calcium release channels in the SR membrane since R_{rel} is the flux of Ca^{2+} and $C_0 - I(t)$ is proportional to the driving force (if the cytosolic $[Ca^{2+}]$ is negligible compared with the intra-SR $[Ca^{2+}]$); for details, see Discussion.

When normalized to SR content, the R_{rel} records (Fig. 5 *C*) from before and after injection for the most part superimposed, the only striking difference being the absence of the early peak after the injection. After correcting R_{rel} for depletion of calcium from the SR (Fig. 5*B*), the record following the injection rose monotonically

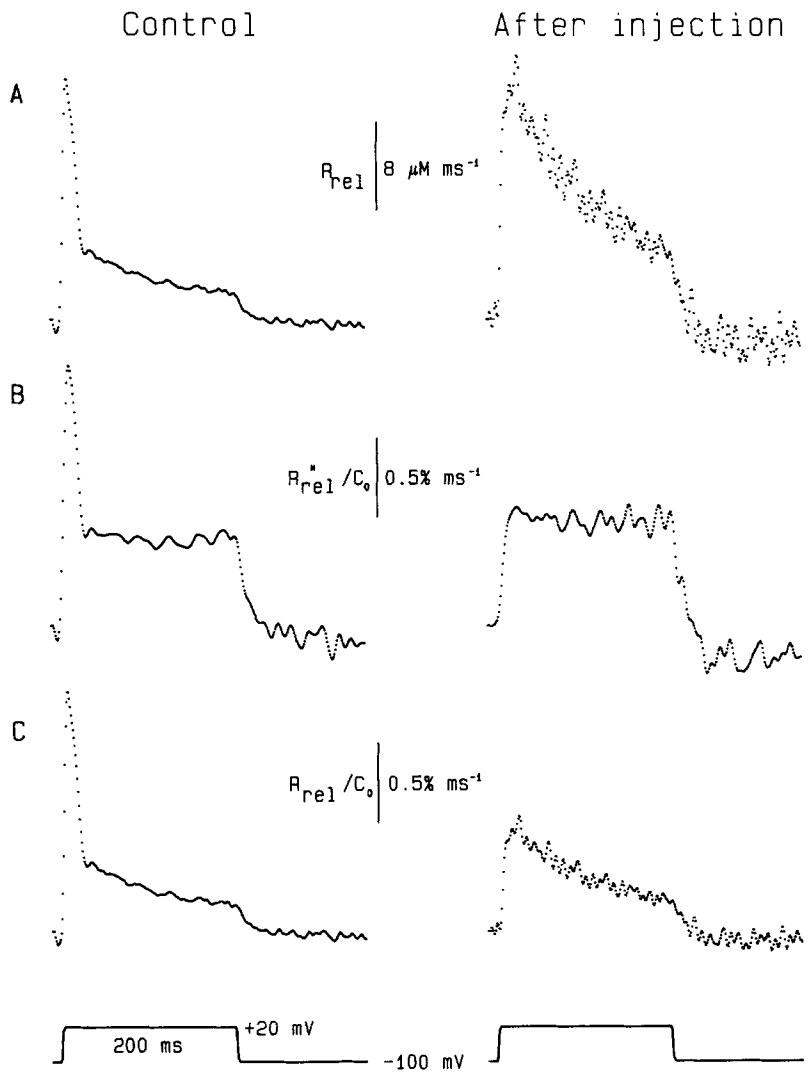

FIGURE 5. (*A*) The rate of release of calcium from the SR (R_{rel}) calculated from the calcium transients measured right before (*Control*) and after the injection. The parameters used to describe the binding of calcium to intracellular calcium binding sites are given in the legend of Fig. 4. (*B*) R_{rel} was corrected for the depletion of calcium from the SR (R^*_{rel}), as described in the text, and normalized to SR contents (C_o) to show the time course of the number of open calcium channels in the SR (see Discussion). The estimated calcium contents of the SR were 1.45 and 3.3 mM, if free in myoplasmic water, before and after injection, respectively. (*C*) To correct for the possible errors in the relative scaling of calcium bound to noninjected sites and injected buffers, and thus enable direct comparison of records from before and after injection (see text for details), R_{rel} is presented as normalized to SR content. Same fiber as in Figs. 2–4.

to a steady level that was the same as the steady level reached in control after the early peak. Since the only difference between the conditions after vs. before injection was the presence of the injected buffer and the absence of the increase in $[Ca^{2+}]$ following the depolarizing pulse, either the activation of the early peak was due to a calcium-dependent mechanism or BAPTA directly and selectively blocked the peak component of calcium release from the SR.

The 2.28-fold greater SR content after compared with before injection in this fiber was among the largest discrepancies found in these experiments. In the 17 fibers included in this study in which strong injections were made, the mean ± SEM ratio of C_0 after to before injection was 1.52 ± 0.21 (range 0.6–3.6). Part of this discrepancy in apparent SR content before and after injection may be due to incorrect values for the removal parameters, as considered in the following section.

Injecting a Nonbuffering BAPTA Analogue Has Little Effect on R_{rel}

To test whether the injection itself or BAPTA directly had any effects on the rate of calcium release from the SR, we injected anisidine, structurally half-BAPTA with a $K_D \approx 1$ mM, into six fibers. Fig. 6 shows results from a fiber where the final concentration of anisidine was 6.7 mM and, due to a higher starting pressure, local swelling (~ 15% increase in fiber diameter) was observed for a short period of time. As the pressure was decreased the fiber rapidly, within a few seconds, regained its original size. The increase in holding current due to impalement was 18.2 nA.

The APIII calcium transient (Fig. 6 *A*) was greater after injection than before, demonstrating that the anisidine, even at this high concentration, had no measurable buffering effect. The simultaneously measured fura-2 fluorescence and the calculated fura-2 saturation (*B*) revealed a 20-nM decrease in resting free $[Ca^{2+}]$ without major changes in the time course of calcium bound to fura-2. Since 111.9 μM fura-2 was coinjected with the anisidine, a slight prolongation of the time for full saturation of fura-2 was expected and indeed observed.

The uptake parameters were determined before injection, as described in connection with Fig. 4, and the predicted decays of the calcium transients after repolarization are shown in Fig. 6 *A* as the continuous smooth curves superimposed on the transients both before and after injection. It is clear that, though the transient after injection was not included in the fit, the parameters described its falling phase reasonably well. This was consistent in all anisidine injections and hence we concluded that the injection itself did not modify the uptake system of the fibers.

R_{rel} was calculated from the APIII calcium transients both before and after injection (Fig. 6 *C*), as described in Methods, and then corrected for depletion of calcium from the SR and normalized to SR contents (Fig. 6 *D*). The estimated content of the SR was 1.95 and 2.30 mM before and after the injection, respectively. Though there was a small suppression of the peak of R_{rel} and R^*_{rel}/C_0 after injection (19% for the latter), the result was clearly different from that obtained when BAPTA was injected.

Other High Affinity Buffers Have an Effect Similar to BAPTA

Since the effects of injecting anisidine and BAPTA were so different, it was of interest to see whether or not other BAPTA analogues with high affinity for calcium would have effects similar to BAPTA.

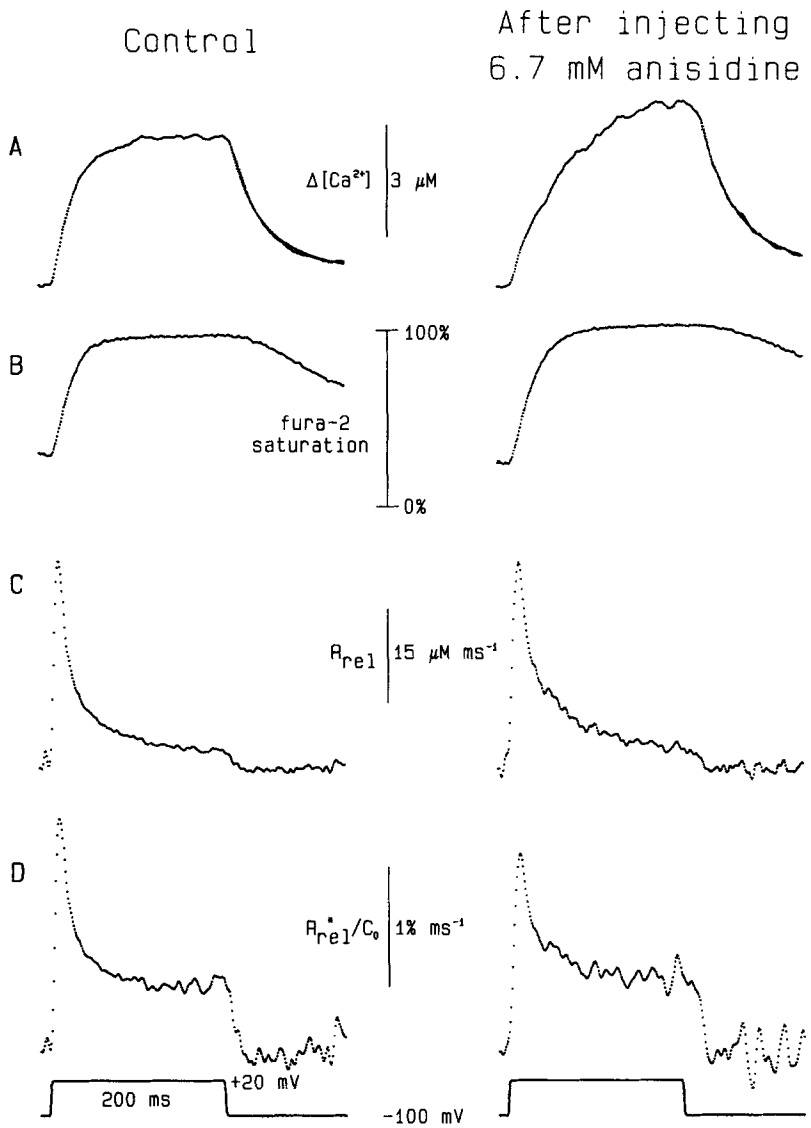

FIGURE 6. The effects of injecting 6.7 mM anisidine on the calcium transient (*A*), the relative saturation of fura-2 (*B*), and the rate of release of calcium from the SR (*C* and *D*). The depolarizing pulse to +20 mV (pulse protocol shown at the bottom of the figure) elicited a calcium transient after injection (*A*, *right*) that was actually greater than that elicited by the same pulse before injection. The removal parameters that described the falling phase of the calcium transient before injection gave a remarkably good fit after injection, too. The predicted decays are shown superimposed on the calcium transients. The time course of the fura-2 saturation (*B*) was essentially unaltered by the injection, although a slight prolongation of the time required to reach full saturation was observed, which was probably due to the higher fura-2 concentration after the injection. The characteristics of the calculated R_{rel} (*C*) were the same before and after injection; both had an early peak followed by a fast and a slow decline. When corrected for depletion of calcium from the SR and normalized to SR content (C_0 = 1.6 and 1.9 mM before and after injection, respectively), the traces (*D*) had a definite peak and then a decline to a steady level. Fiber 924, pl = 65 μm, V_h = −100 mV; injection pipette contained 30 mM anisidine.

Fig. 7 demonstrates the effects of 2.5 mM fura-2 (*A*), 10.6 mM Br_2BAPTA (*B*), and 7.0 mM F_2BAPTA (*C*) on R_{rel} and R^*_{rel}, both normalized to SR content. In the case of Br_2- and F_2BAPTA, the injections with the highest intracellular buffer concentrations are shown. The results of the fura-2 and Br_2BAPTA injections were identical to those obtained with BAPTA; namely, the early peak of R_{rel} was eliminated by the injection

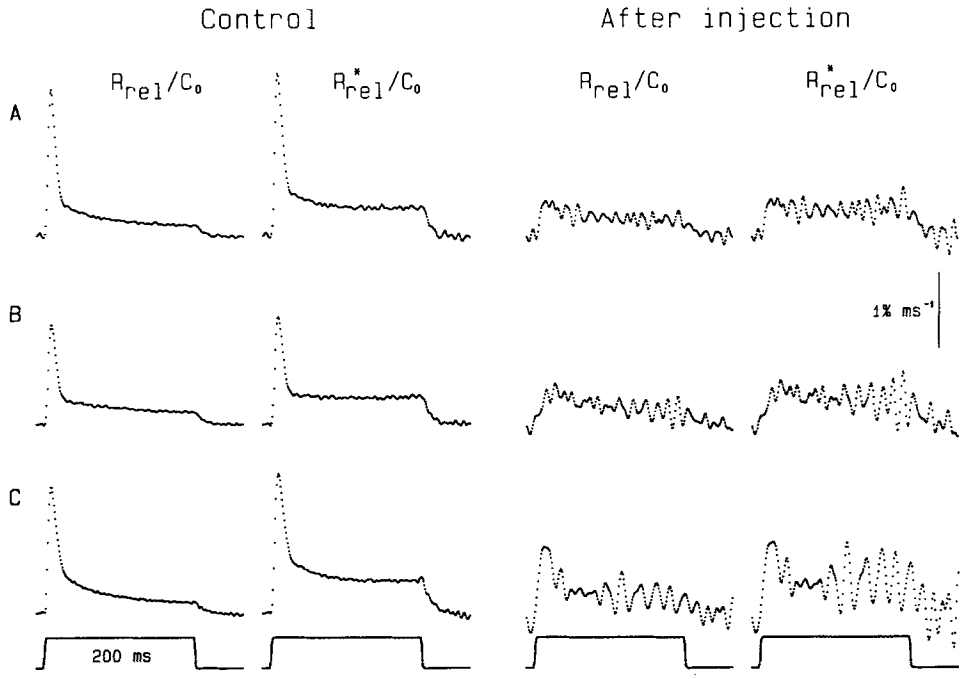

FIGURE 7. The suppression of the peak of R_{rel} after the injection of different affinity calcium buffers. R_{rel} was calculated from the calcium transients measured right before and after the injection of 2.5 mM fura-2 (*A*), 10.6 mM Br_2BAPTA (*B*), and 7.0 mM F_2BAPTA (*C*) (in the order of decreasing affinity). The traces presented were all normalized to the SR contents with C_o = 1.4 and 0.85 mM, 1.7 and 1.5 mM, and 2.9 and 3.2 mM before and after injection for *A*, *B*, and *C*, respectively. After the injection of fura-2 (*A*) and Br_2BAPTA (*B*) the early peak of both R_{rel}/C_o and R^*_{rel}/C_o was eliminated, whereas the injection of F_2BAPTA suppressed but did not completely eliminate the peak. The records after injection are noisy, especially that measured after the injection of F_2BAPTA, most of which arises from the type of calculation used (see Discussion for details). Note that the same vertical scale is used for all fibers. Pulse protocol is shown at the bottom. Fibers 845, 838, and 854, pl = 78, 77, and 77 μm, respectively, V_h = −90 mV, and V_{test} = +10 mV for all three fibers.

but the steady levels, calculated from R^*_{rel}/C_0, were the same before and after injection. There seems to be a small peak present in the records measured after the injection of F_2BAPTA. This was consistent with the fact that the underlying calcium transient was not completely suppressed after the F_2BAPTA injection, having a peak value of 0.6 μM (not shown). It should also be noted that the scale is the same for

each record in Fig. 7. Although the peaks of R^*_{rel}/C_0 varied considerably, the steady levels, which represent the number of channels attributable to the noninactivatable component of release, seemed to be relatively constant from fiber to fiber.

An obvious difference between the records before and after injection in Fig. 7 was that the latter had considerably more noise. A detailed account of the origin of this noise is given in the Discussion.

Fig. 8 presents the average effect of the injections of anisidine (*A*) and the high affinity buffers (*B*) on the peak and steady levels of R^*_{rel}/C_0. All injections where the increase in $[Ca^{2+}]$ was greater than 300 nM during the depolarizing pulse after

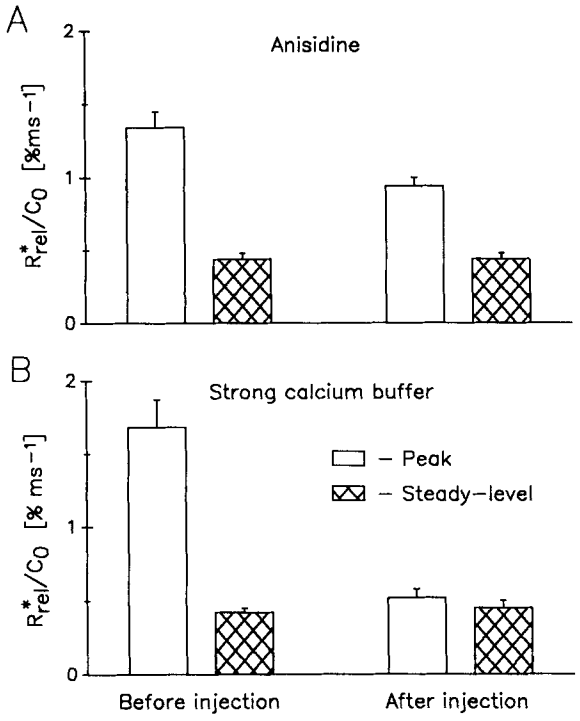

FIGURE 8. Differential effects of anisidine (*A*) and high affinity buffer (*B*) injections on the waveform of R^*_{rel}/C_0. The values presented are the average of 6 injections with anisidine and 17 injections with the other buffers. No selection was made among the anisidine injections (an injection where the resting $[Ca^{2+}]$ increased by 400 nM was included in the average) to emphasize any damage that might have been the result of the injection. The 17 injections with high affinity buffers were selected to fulfill the criteria that the increase in $[Ca^{2+}]$ during a 200-ms depolarizing pulse to >0 mV was not greater than 300 nM and the concentration of the injected buffer was at least 2 mM. The peak of R^*_{rel}/C_0 was calculated as the greatest value in the first 50 ms, whereas the steady level is the average of the values in the last 50 ms of the depolarizing pulse. Note that this method overestimates the peak since it tends to include part of the noise into the value of the peak. The error bars represent the SEM.

injection (that is, all F_2BAPTA injections) were left out of the average when the effects of high affinity buffers were calculated. The steady level of R^*_{rel}/C_0 was not significantly modified by the injection of either anisidine ($P > 0.9$) or the high affinity buffers ($P > 0.5$). Although the peak R_{rel} was partially suppressed after the injection of anisidine, by 26% on average, it was still considerably greater than the steady level (2.14 times). The injection of the high affinity buffers, on the other hand, completely eliminated the peak, resulting in records where the steady level was not significantly different ($P < 0.3$) from the peak, considering that the peak was calculated as the greatest value in the first 50 ms, i.e., including part of the noise,

while the steady level is the average of the values of the last 50 ms during the depolarizing pulse. The values in Fig. 8 and all release records presented in this paper were for large depolarizations that maximally activated release. However, peaks in R_{rel} records for smaller pulses were also selectively eliminated by strong injections of calcium buffers.

The conclusion is that neither the injection per se nor the chemical structure of BAPTA is likely to be responsible for the elimination of the peak of R_{rel}. This leaves only the possibility that the suppression of the myoplasmic calcium transient to nanomolar levels was responsible for the above changes; that is, the inactivatable component of R_{rel} was activated by the local increase in $[Ca^{2+}]$.

Changes in Electrical Properties Due to the Injection

There was an increase in the holding current in all injections (by 61.1 ± 15.3 nA; mean ± SEM, $n = 41$) due to the impalement and microinjection. For the holding voltage of −100 mV the mean increase in holding current corresponds to a mean leak resistance of ~2 MΩ at the electrode impalement site due to the impalement and microinjection. In 68% of the cases the holding current decreased after removing the electrode, sometimes nearly to preinjection levels. For the six anisidine injections (included in the above) the mean increase in holding current was 73.9 ± 50.5 nA. Thus the anisidine injections, which did not eliminate peak calcium release, produced about the same leak conductance as strong injections that did eliminate peak release.

Fig. 9, *A* and *B*, presents total current records for 200-ms depolarizing pulses to +20 mV in two different fibers before and after microinjection. The records in Fig. 9 *A* are from the same fiber and pulses as used for the calcium transients in Fig. 3. In this fiber before injection (Fig. 9 *A, control*) the initial outward capacitative transient at the start of the pulse was followed by an outward current that increased slightly with time during the 200-ms pulse. At 2 min after injection the steady outward current for the same pulse was increased, presumably due to the added leak conductance at the impalement site, and the time-dependent increase in outward current was absent. At 3 min after injection the outward current during the pulse had decreased and at 25 min (not shown in Fig. 9 *A* so as not to obscure the control record) the steady current was about the same as control, indicating a major recovery from the electrode impalement leak.

Fig. 9 *B* shows current records from a different fiber in which the steady current during the depolarizing pulse was actually slightly less 4 min after injection than in control. Since the APIII calcium transient and the early peak component of R_{rel} were eliminated in both fibers (Fig. 9 *A*: Figs. 2–4; Fig. 9 *B*: Figs. 1 and 2 of Jacquemond et al., 1991*a*), an increased outward current was not necessary for the elimination of the calcium transients. As in Fig. 9 *A*, the control current record in Fig. 9 *B* also appears to include a small time-dependent increase in outward current during the pulse that was absent after injection. Also, both fibers exhibited a slow tail of inward current after the pulse in control that was absent after injection. In the fiber in Fig. 9 *B*, currents were also recorded for 20-mV hyperpolarizing pulses (100-ms duration; records not shown). The current for the −20-mV pulses was increased after injection, presumably due to the electrode impalement leak. The short record in Fig. 9 *B* is the

current record for the depolarizing pulse after injection, corrected for the change in leak current (obtained as the difference in current for the −20-mV pulses before and after injection scaled by the ratio of the depolarizing and hyperpolarizing pulse amplitudes). This procedure should remove the change in leak current after the injection since the leak should be linear.

Fig. 9 *C* gives the difference in the control and the corrected postinjection records from Fig. 9 *B*. It indicates that a time-dependent outward current, presumably calcium activated, was abolished by an injection of BAPTA that completely eliminated

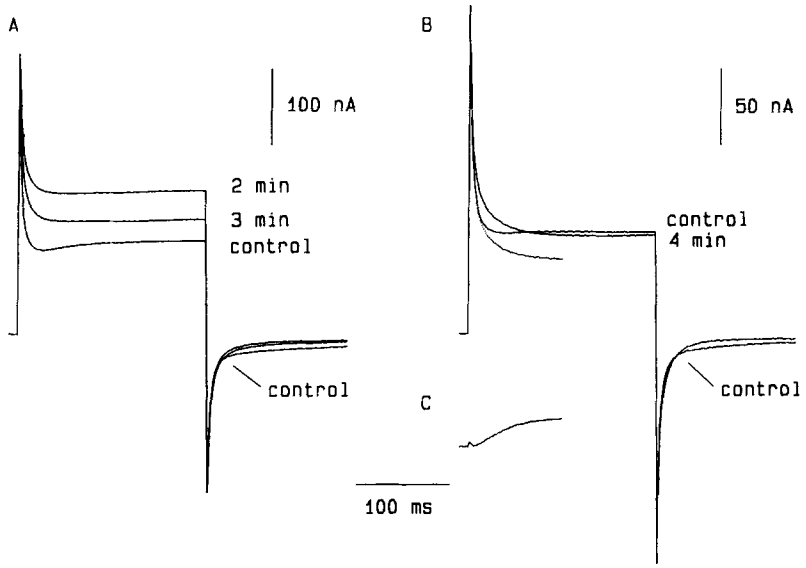

FIGURE 9. Effect of injecting strong calcium buffers on total currents for pulses to +20 mV in two different fibers. (*A*) Total fiber current for a 200-ms depolarizing pulse to +20 mV before injection (control) and 2 and 3 min after injection of 5.8 mM BAPTA. Same fiber and pulse applications as in Fig. 3. (*B*) Total fiber current for a 200-ms pulse to +20 mV (full records) before injection (*control*) and 4 min after injection of 4.1 mM BAPTA into another fiber. The shorter (partial) record gives the initial 110 ms of the postinjection record corrected for the change in leak current due to injection, which was obtained as the difference in current for 20-mV hyperpolarizing pulses (100 ms) applied before and after injection scaled by the ratio of the depolarizing and hyperpolarizing pulse amplitudes. Same fiber as in Figs. 1 and 2 of Jacquemond et al., 1991*a*. (*C*) The current in control in *B* that was eliminated by the microinjection, obtained as the control current in *B* minus the corrected postinjection record.

the APIII calcium transient in this fiber. Although the small initial outward transient in Fig. 9 *C* might be taken to indicate a small component of charge movement that was also suppressed by the injection, records similar to Fig. 9 *C* but lacking the initial transient were obtained from a second fiber in which current was recorded for −20-mV pulses and in which the BAPTA injection again completely eliminated the calcium transients (records not shown). Thus, a change in charge movement did not appear to be involved in the changes in calcium transients and R_{rel} produced by strong BAPTA injections. Finally, in a third (and last) fiber in which current was

monitored for −20-mV pulses, the change in current after injection was eliminated entirely by the correction for the change in leak current. The calcium transients and early peak in R_{rel} in this fiber were again completely suppressed by the BAPTA injection, indicating that suppression of a time-dependent outward current was not necessary for the BAPTA effect. This last fiber contained potassium instead of cesium as the predominant cation in the internal solution, which might be expected to promote calcium-activated K^+ current; yet, surprisingly, no time-dependent outward current was detected before injection. Since only a single fiber was examined under these conditions using hyperpolarizing pulses before and after injection, it is not known whether the absence of time-dependent outward current in this fiber before injection was due to fiber to fiber variation or to the different internal cation.

In summary, the overall conclusion from examination of current records is that the suppression of calcium transients and the early peak of R_{rel} were not due to changes in fiber electrical properties produced by the injection, although the injections did produce a leak conductance and did suppress a time-dependent outward current in most fibers.

Alternative Parameters for the "Intrinsic" Calcium Binding Sites

Close examination of the R_{rel}, especially the R^*_{rel} record, after injection in Fig. 5 revealed another difference between the traces obtained before and after the injection: namely, an undershoot below baseline (that is, to negative values) after repolarization. The undershoot was more pronounced after correcting for depletion since $C_0/[C_0 - I(t)]$, the multiplicand to obtain R^*_{rel} from R_{rel}, monotonically increases with time and is always greater than 1. We attributed the undershoot to an incorrect removal prediction after injection, presumably arising from the fact that the removal parameters obtained before injection did not describe the system after the injection. Since the removal parameters were not changed in injections without calcium buffer (Fig. 5) there was no reason to believe that the injection process itself should change these parameters. This implies that the original removal parameters might be wrong.

Fig. 10 considers three alternative attempts (rows *A*, *B*, and *C*) to describe the removal of free calcium from the myoplasm after repolarization. The first and third columns of Fig. 10 show the measured calcium transients and the predicted decays of $\Delta[Ca^{2+}]$ (less noisy traces). The second and fourth columns present, respectively, calcium bound to the noninjected sites ($\Sigma_i[Ca\text{-}S_i]$) before and the calcium bound to the injected buffers ([Ca-B]) after injection. Fig. 10 also presents the amount of calcium transported back into the SR via the calcium pump (traces labeled P) before and after injection (second and fourth columns, respectively). As shown in connection with Fig. 4, $\Sigma_i[Ca\text{-}S_i]$ + P and [Ca-B] + P represent the major components of calcium uptake before and after the injection, respectively. The time scale in Fig. 10 was compressed to allow the comparison of the measured and predicted decays of the calcium transients during an almost 2-s interval after the pulse. On the other hand, the vertical scale for $\Delta[Ca^{2+}]$ before injection was expanded in order to visualize the late events, which resulted in most of the points of the transient being off scale during and shortly after the pulse.

For Fig. 10*A* the calculations were done using the removal parameters determined with the fits presented in Fig. 4. It is clear that the predicted decay of the calcium transient was much slower than measured, reaching a discrepancy of ~20% by the

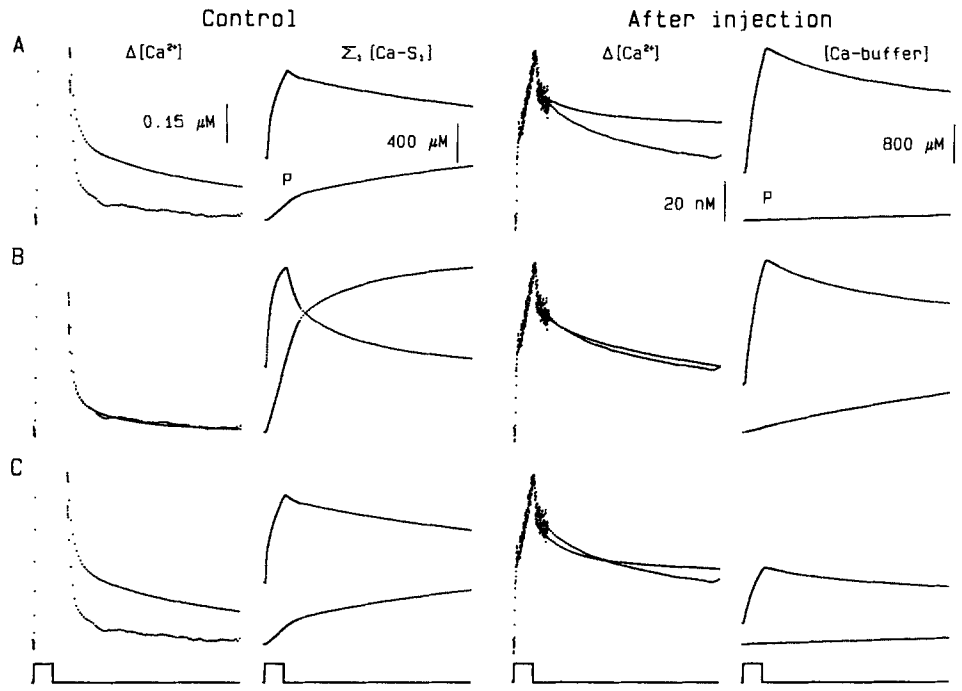

FIGURE 10. Alternative ways to describe the decay of the calcium transient following repolarization measured after injection. Three different sets of values for the calcium binding to noninjected sites or injected buffers were considered and the results are presented in rows *A*, *B*, and *C*. Columns labeled $\Delta[Ca^{2+}]$ present the measured calcium transients (noisier traces) and the superimposed predicted decays (noiseless traces), whereas columns two and four show the calcium bound to the noninjected sites and to the injected buffers, respectively, for each different removal prediction. The traces labeled *P* (in the second and fourth columns) show the calcium transported back into the SR via the SR calcium pump. Note that the time scale is different compared with all other figures to show an almost 2-s interval from the decay of the calcium transients. (*A*) Traces calculated with the parameters described in connection with Fig. 4, i.e., using the pulses to −20 mV from before injection to obtain the removal parameters. (*B*) The trace after injection was included in the fit together with those for three pulses to −20 mV before injection shown in Fig. 4 *A* and the properties of the noninjected sites were allowed to change to give the best fit. The parameters that had to be changed compared with *A* are [parvalbumin] = 1,280 μM, $k_{off,Mg\text{-}parvalbumin}$ = 8.0 s^{-1}, PV_{max} = 4,687 μM s^{-1}, and [troponin C] = 880 μM. Although not included into the fit, the decay of the calcium transient before injection was extremely well predicted (*B, first column*). (*C*) Including the calcium transient from after injection into the fit as in *B* and using the same removal parameters as in *A*, the concentration of the injected buffers were set to obtain the best fit. The fitted value of the sum of the concentrations of fura-2 and BAPTA was 2,470 μM, 40.1% of that originally calculated (and used in *A* and *B*). For further details see text. Same fiber as in Fig. 2.

end of the sampled period after injection (third column). Although the absolute difference between the measured and the predicted decay of $\Delta[Ca^{2+}]$ was actually greater before (first column) than after the injection, it only represented 2.5% of the overall $\Delta[Ca^{2+}]$ before injection. The calculated R_{rel} should thus show a relatively greater undershoot after injection than before, as observed (Fig. 5 *A*).

To improve the fit to the decay of $\Delta[Ca^{2+}]$ after injection, we included the calcium transient for the pulse after injection in the fit. There were then two different methods of correcting for the discrepancy between the predicted and measured decays of $\Delta[Ca^{2+}]$ after injection. One was to assume that the removal parameters determined before injection were incorrect and thus try to adjust them to obtain a better fit. This was done in Fig. 10 *B*. The other was to keep the removal parameters the same and adjust the concentration of the injected buffer so as to get a better fit after injection (Fig. 10 *C*). There are problems with both methods, as discussed in detail in the Discussion. The first might lead to parameters not supported biochemically, whereas the latter will not correct the fit before injection.

Using the record from after injection, including the 1.8-s part shown in Fig. 10 *A*, and the three records to −20 mV from before injection (Fig. 4 *A*), the removal parameters were recalculated, yielding the fits presented in Fig. 10 *B*. Though not included in the fit, the decay of the calcium transient measured just before injection (Fig. 10 *B*, first column) was extremely well predicted. The difference between the removal parameters used in Fig. 10, *A* and *B*, was mainly an increase in the total concentration of the calcium-specific sites of troponin C, which resulted in a similar change in PV_{max} and a decrease in the total concentration of parvalbumin. Before injection these changes resulted in a slightly greater amount of calcium bound to the noninjected sites (894 vs. 1,030 μM in Fig. 10, *A* and *B*, respectively) at the end of the pulse and significantly more calcium transported back to the SR by the pump (161 vs. 710 μM). After injection, although similar changes occurred, they were negligible when compared with the amount of calcium bound to the injected buffers (Fig. 10 *B*, fourth column).

In an alternative approach, the decay of the calcium transient after injection could be described if the concentration of the injected buffer was assumed to be only 40% of that actually calculated (Fig. 10 *C*). The fits, even that after injection, were, however, not as good as in Fig. 10 *B*. The calcium bound to the noninjected sites and that transported by the pump was, naturally, the same as in Fig. 10 *A*, both before and after injection, since no change was made in any removal parameter value, whereas the calcium bound to the injected buffers decreased to 40% of its original value, that is, from 2.31 mM to 923 μM.

It is interesting to note that in both cases (Fig. 10, *B* and *C*) the calculated total amount of calcium released before injection became closer to that released after injection. If compared with the original case (Fig. 10 *A*), when the removal parameters were adjusted (Fig. 10 *B*) the calculated calcium released before injection increased (from 1.08 to 1.75 mM), whereas that after injection stayed almost constant (2.48 and 2.70 mM for Fig. 10, *A* and *B*, respectively). The opposite occurred when the concentration of the injected buffers was decreased (Fig. 10 *C*): the calculated calcium released stayed constant before injection and decreased (from 2.48 to 1.10 mM for Fig. 10, *A* and *C*, respectively) after injection.

Fig. 11 presents the release records calculated before and after injection for the case when the removal parameters were adjusted (as described above, Fig. 10 *B*) to give a better fit to the decay of the calcium transient after injection. The overall kinetics of the R_{rel} records in Fig. 11 *A*, from both before and after injection, were essentially the same as the records calculated with the original fit (presented in Fig. 5 *A*), apart from the fact that the undershoot was missing from the trace calculated

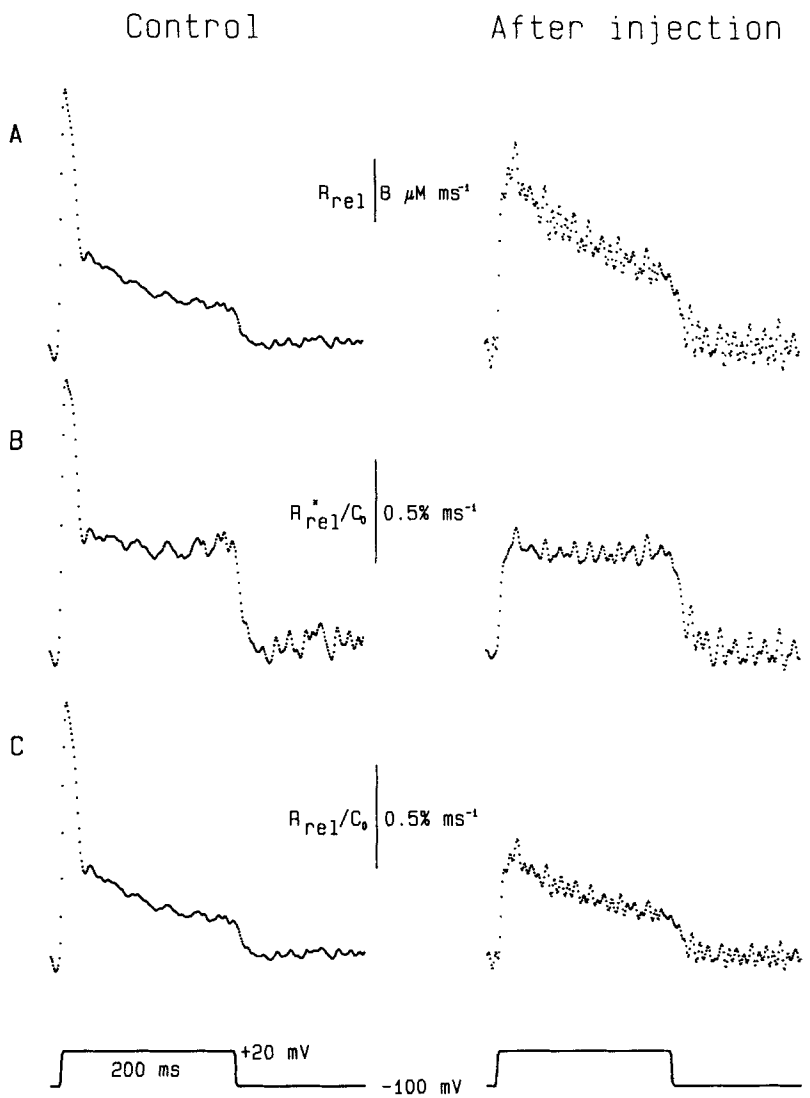

FIGURE 11. (*A*) R_{rel} before and after injection recalculated with the removal parameters obtained when the calcium transient from after injection was included into the fit (Fig. 10 *B*). The most noticeable difference compared with Fig. 5 was the change in the relative size of the records: the R_{rel} after injection became smaller than the R_{rel} before injection. (*B*) R_{rel} corrected for depletion of calcium from the SR and then normalized to SR content. C_o = 2.6 and 4.5 mM before and after the injection, respectively. (*C*) When R_{rel} records were normalized to SR contents to enable direct comparison of the traces obtained before and after injection, they showed the same characteristics as in Fig. 5. Same fiber as in Figs. 2–5 and 10.

after the injection in Fig. 11 *A*. Furthermore, the general conclusion, that after normalizing to SR content the R^*_{rel} and R_{rel} (Fig. 11, *B* and *C*, respectively) lost their peaks due to the injection with no change in the steady level, remained the same. There were minor quantitative changes: namely, the peak and the steady level were

smaller with the adjusted removal parameters (1.64 and 1.30 for the peak and 0.57 and 0.52 for the steady levels, with the parameters for Fig. 10, *A* and *B*, respectively; the values correspond to the trace from before injection). Similar results (not shown) were obtained if the concentrations of the injected buffers were assumed to be smaller (see above, Fig. 10 *C*), only the absolute values were even closer to the originals.

Carrying out similar fits and calculations in other fibers, the overall result was that if the estimated SR calcium content was higher after injection than before, as in the fiber in Fig. 10, the adjustment of the removal parameter values required to obtain a reasonable fit after injection also resulted in bringing the calculated contents closer before and after injection. In other fibers in which the estimated contents were about the same before and after injection to begin with, the original fit to the records before injection generally described the decay of the calcium transient after the injection reasonably well. We thus concluded that even though the relative scaling of the noninjected vs. injected sites in some fibers might have been wrong, the normalization of R_{rel} or R^*_{rel} to the estimated SR calcium content should have, for the most part, corrected this problem. All the analysis above thus used the removal parameters calculated from fits to the decay of $\Delta[Ca^{2+}]$ from 15 to 115 ms after the pulses to −20 mV before injection.

DISCUSSION

Calcium-induced Calcium Release in Skeletal Muscle

The results presented in this article show that the microinjection of high affinity buffers into voltage-clamped cut skeletal muscle fibers selectively inhibits the early peak component of the rate of calcium release from the SR (Figs. 5 and 7). The effect seemed not to be a direct consequence of the injection itself (see below for further discussion on this point), and only depended on the suppression of the myoplasmic calcium transient. This observation implies a dual control of the release process, as suggested by Ríos and Pizarro (1988): namely, the presence of a membrane voltage-operated and a $[Ca^{2+}]$-dependent component. The source of the calcium that is needed to activate the latter is probably the SR; that is, the calcium released through the voltage-operated channels, the opening of which depends on the movement of intramembrane charges, serves as the triggering stimulus.

In the framework of this model, the absence of sizable calcium transients would prevent the activation of the calcium-induced component and lead to a decreased R_{rel}. The interpretation of the present data would thus be that the noninactivatable component of R_{rel}, which gives rise to the steady level, is voltage operated and that the inactivating, or peak, component of R_{rel} is due to a calcium-induced calcium release mechanism. Recently, Pizarro et al. (1992) reported that tetracaine, a drug shown to suppress calcium-induced calcium release, selectively blocked the peak component of R_{rel}, providing further evidence in favor of the dual control model.

On the other hand, the suppression of the peak of R_{rel} is in direct contrast to the findings of Baylor and Hollingworth (1988) and Hollingworth et al. (1992), who observed an enhancement of calcium release in intact fibers injected with fura-2 and stimulated with action potentials. In those experiments, however, the injection of several millimolar fura-2 was insufficient to buffer the increase in $[Ca^{2+}]$ to nanomolar levels after an action potential, and this might have resulted in the activation of

the calcium-induced component. Apparently, more calcium was released or the injected buffer was less effective (or both) in the experiments of Hollingworth et al. (1992) than in the present experiments. Although the reason for this difference between intact, action potential–stimulated fibers and cut voltage-clamped fibers is unclear, it does not appear to be due to cutting the fibers. Intact fibers voltage clamped in our double Vaseline gap chamber and injected with APIII and fura-2 gave $[Ca^{2+}]$ transients similar to cut fibers (Jacquemond, V., and M. F. Schneider, unpublished observations).

Dissociation Constants for the Calcium–Buffer Reaction

The available data on the apparent dissociation constants of the high affinity buffers used in this study are relatively diverse. Values for the intracellular solution of intact cells are almost nonexistent.

The best documented is fura-2. Previous studies (Baylor and Hollingworth, 1988; Klein et al., 1988) using APIII and fura-2 simultaneously to monitor changes in intracellular $[Ca^{2+}]$ presented $k_{on,f}$ and $k_{off,f}$ values close to those found in this study. Although these $k_{on,f}$ and $k_{off,f}$ values are smaller than those obtained in cuvette measurements (see, for example, Kao and Tsien, 1988), they probably represent a close estimation of the actual values valid intracellularly. The calculated dissociation constant, however (average $K_{d,f}$ = 113 nM, this study), is fairly close to values from cuvette measurements (Grynkiewicz, Poenie, and Tsien, 1985; Kao and Tsien, 1988).

The dissociation constant of BAPTA is believed by most authors (Tsien, 1980; Haugland, 1989) to be somewhat lower than that of fura-2, but counter examples do exist (Pethig, Kuhn, Payne, Adler, Chen, and Jaffe, 1989). The range of reported values for $K_{d,BAPTA}$ is 100–700 nM (Tsien, 1980 and Pethig et al., 1989, respectively), depending on ionic strength and temperature. The cuvette calibrations closest to our conditions are those of Harrison and Bers (1987), who examined, among others, the effects of low temperature and obtained a value of ~400 nM for the $K_{d,BAPTA}$ at 12°C (value read from Figs. 4 and 6 of that study). We used identical rate constants for the calcium-fura-2 and calcium-BAPTA, which was the most straightforward approach but which might have overestimated the actual dissociation constant of BAPTA in the myoplasm. The effects of using alternative rate constants are discussed in the following section.

Although the values that can be found in the literature for the dissociation constants of Br_2BAPTA and F_2BAPTA are as diverse as for BAPTA, less data are available. All are consistent in that F_2BAPTA has the lowest affinity of the four compounds studied here, having a dissociation constant ~8–10 times that of fura-2 (Pethig et al., 1989; Smith, Hesketh, Metcalfe, Feeney, and Morris, 1983), whereas the dissociation constant for Br_2BAPTA is believed to be about four to six times that of fura-2 (Harrison and Bers, 1987; Pethig et al., 1989). The values used in this study, 1.58 and 2.45 μM for Br_2BAPTA and F_2BAPTA, respectively, represent those given by Molecular Probes, Inc. (Haugland, 1989) and probably likewise overestimate the actual values in the myoplasm.

The rate constant $k_{on,B}$ is likely to be the same for the different buffers, since it approaches the diffusion limit ($> 10^8$ $M^{-1}s^{-1}$), so that $k_{off,B}$ has to be different. This was assumed throughout the paper.

Elimination of the Peak R_{rel} Was Not Due to the Assumption Concerning the Calcium Buffer

Since after a strong injection most of the calcium released from the SR is bound to the injected buffers (~90–95%; see Fig. 4), the kinetics of R_{rel} critically depend on the assumed time course of calcium binding to these sites. In the case of the fura-2 injections, where the dye and the buffer were the same so that the calcium bound to the buffer was directly measured, this was not a problem. It is conceivable, however, that when any other buffer was injected the rate constants for the calcium–buffer reaction in the fiber were different from those used in the calculations. We thus tested whether the loss of the peak of R_{rel} might be due to the calculation of calcium bound to BAPTA. Assuming that the same release as measured before injection also took place under the postinjection conditions, we predicted the free $[Ca^{2+}]$ transient and the calcium binding to the noninjected sites, to fura-2, and to BAPTA, using the parameters determined before injection and several alternative $k_{on,B}$ and $k_{off,B}$ values for the calcium–BAPTA reaction.

On the basis of the previous section we assumed that BAPTA has the same or higher affinity for calcium than does fura-2. Fig. 12 shows the predicted calcium transients when $k_{on,B}$ was set equal to $k_{on,f}$ (*A*) or when $k_{on,B}$ was twice $k_{on,f}$ (*B*) with the dissociation constant of BAPTA equal to (left column) or half of (right column) the value for fura-2. The most striking difference between the predicted (*A* and *B*) and measured (lowermost trace) calcium transients is the presence of an early peak in all of the predicted records. When $k_{on,B}$ was smaller than $k_{on,f}$ (not shown in the figure), the peak in the predicted calcium transient was even more pronounced. Assuming that R_{rel} can be approximated by the change in calcium bound to the high affinity buffer (see Eq. 4a) and that the dissociation rate of calcium from the buffer can be neglected compared with the association rate at early times (see Eq. 3), $R_{rel} = k_{on,B} \cdot [B]_T \cdot \Delta[Ca^{2+}]$. The calcium transient in a heavily buffered system should thus be proportional to the rate of release and inversely proportional to the association rate of the buffer (Rios and Pizarro, 1991). The fact that "peaky" calcium transients were never observed after strong injections argues strongly against any possible peak in R_{rel} after injection.

Note that the scales for the measured and the predicted calcium transients are different. There was also a difference in the estimated SR calcium contents before and after injection (see Fig. 5), which renders the comparison of the calcium transients predicted from R_{rel} before injection with the calcium transient measured after injection difficult. Nevertheless, a simple scaling of R_{rel} before injection with the ratio of the SR contents resulted (data not shown) in predicted calcium transients that had similar shapes to those in Fig. 12, but in which the slowly rising phase after the early peak and the decline after the termination of the pulse were comparable in size to the one actually measured.

The calcium transients predicted using the various assumed values of $k_{on,B}$ and $k_{off,B}$ were used to calculate the predicted R_{rel} after injection with the procedure described in Methods and used in Results. That is, the calcium bound to BAPTA was calculated with $k_{on,B}$ and $k_{off,B}$ not equal to the various values used in making the predictions but rather always set equal to the values used for fura-2. In other words, we tested

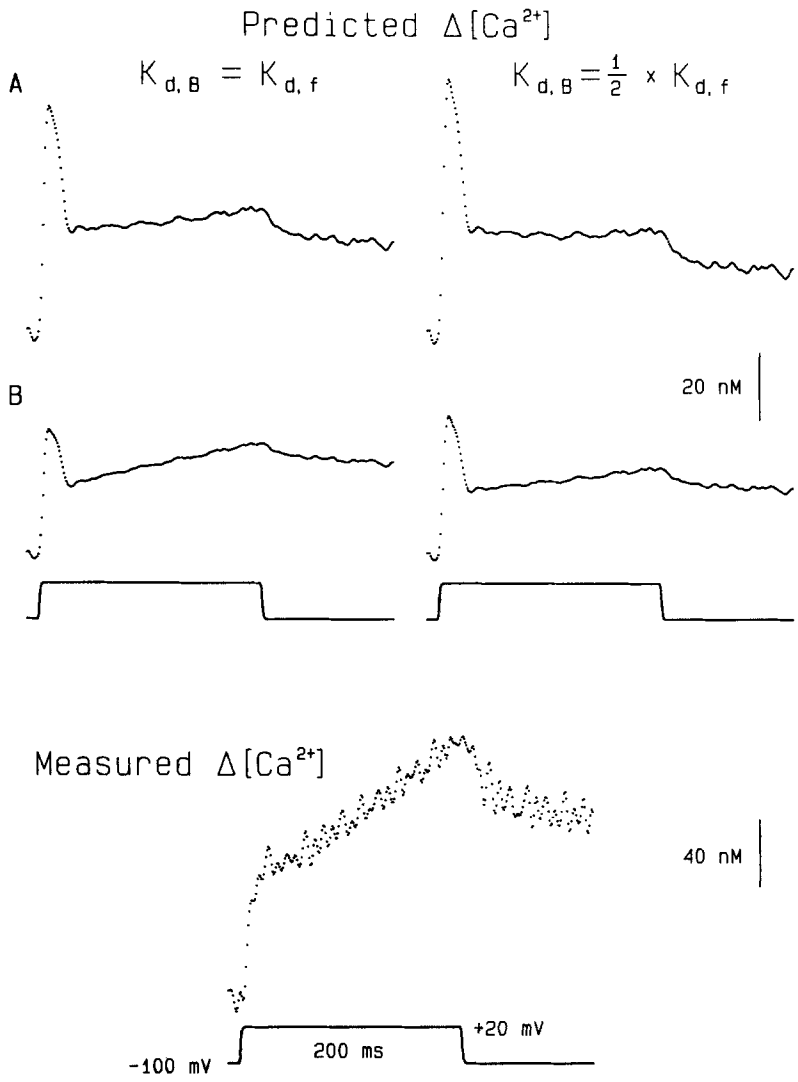

FIGURE 12. Comparison of predicted and measured calcium transients after injection. Assuming that the calcium release measured before injection happened in the postinjection conditions, that is, when the injected BAPTA and fura-2 were also present, the change in free calcium concentration was predicted using different rate constants for the calcium-BAPTA reaction (*Predicted* $\Delta[Ca^{2+}]$). In the prediction $k_{on,B}$ was either equal to $k_{on,f}$ (*A*) or $k_{on,B}$ was twice $k_{on,f}$ (*B*) with the dissociation constant of BAPTA either equal to or half that of fura-2. The parameters of the removal system were the same as those given in the legend of Fig. 4, while the rate constants for the calcium-fura-2 reaction are given in the legend of Fig. 2. For comparison, the calcium transient calculated from the measured fluorescence signal is shown as the lowermost trace (*Measured* $\Delta[Ca^{2+}]$; same as in Fig. 4).

whether or not using different rate constants in the prediction and in the calculation would attenuate the assumed peak of R_{rel}.

Naturally, if equal affinity was used with equal rate constants, the calculated R_{rel} was essentially identical to the R_{rel} used for the prediction, providing a direct control of the calculations themselves. If the rate constants were decreased or increased by the same factor while maintaining $K_{d,B} = K_{d,f}$, the peak of R_{rel} increased or decreased, respectively.

When the affinity of BAPTA was increased in the calculation by making $k_{off,B}$ smaller than $k_{off,f}$ with the forward rate constants being the same, the calculated R_{rel} was actually more peaky than the assumed; i.e., its peak to steady level ratio increased. On the other hand, when the affinity of BAPTA was increased by making $k_{on,B}$ larger than $k_{on,f}$ the peak decreased. Doubling $k_{on,B}$ resulted in a 30% decrease in the peak to steady level ratio.

In general, the observation was that the underestimation of $k_{on,B}$ in the R_{rel} calculation would have resulted in an underestimation of the peak, if there was any, whereas any discrepancy in $k_{off,B}$ would not have affected our conclusion that the presence of high intracellular buffer concentrations eliminate the peak of R_{rel}. Since the k_{on} values for all these buffers are mainly diffusion limited, the underestimation of $k_{on,B}$ by several fold, which would have been necessary to account for the total loss of the peak, is highly unlikely.

Elimination of the Peak R_{rel} Was Not Due to the Injection Itself

Hollingworth et al. (1992) suggested that the suppression of the released calcium after the injection of several (>6) millimolar fura-2 might be the result of damage caused by the injection. They argued that the suppression was only seen at the site of the injection, that it was accompanied by a prolongation in the time course of the calcium release, and that this prolongation recovered rapidly with time.

In our experiments, successful injections increased the latency of the fura-2 fluorescence change by ~2 ms, but this increase did not change significantly during recovery (Fig. 3 and related text). Sometimes even when the holding current increased dramatically and/or visible damage was seen at the point of microelectrode penetration, the latency of the signal remained about the same though the rate of rise of the calcium transient, and consequently the peak R_{rel}, decreased. When visible damage without any change in latency happened in anisidine injections it was accompanied by a drastic increase in resting $[Ca^{2+}]$ and slowing down of calcium removal from the myoplasm after a depolarizing pulse. When strong buffers were injected, such changes in $[Ca^{2+}]$ were prevented by the presence of the buffer.

A direct test for injection damage would be the inability to inject similar amounts of nonbuffering saline without suppressing the peak component of R_{rel}. This was not the case since anisidine could be injected, without major changes, to concentrations comparable with those of the high affinity buffers. We thus concluded that the elimination of the peak R_{rel} observed in the experiments using high affinity buffers was not due to the injection process. Although we cannot rule out the possibility of a small difference in the charge of osmolarity or ionic strength after the injection of similar concentrations of strong buffers and anisidine, it seems highly unlikely that

the elimination of peak R_{rel} by injection of strong buffers but not by anisidine would be due to such an effect.

There was, nevertheless, some decrease in the peak of R_{rel} after the injection of anisidine. This has to be attributed to damage caused by the injection itself, though some contribution from the fiber run-down which would have taken place without the injection cannot be ruled out. Since the increase in free $[Ca^{2+}]$ near the release sites during the pulse was smaller after injection than before (R_{rel} was smaller), the decrease in peak release cannot be accounted for by a larger or faster development of inactivation during the pulse. The mechanism underlying the suppression of peak R_{rel} was unlikely to be the inactivation of voltage sensors since the steady release, which is graded by charge movement (Simon and Schneider, 1988; Simon and Hill, 1992), was not decreased. A local increase in resting $[Ca^{2+}]$ near the injection site could, on the other hand, lead to a calcium-dependent inactivation of the release channels before the pulse and account for the reduction in peak R_{rel}. In the framework of the dual activation model this means that some of the channels that would have been activated by calcium were already inactivated before the depolarizing pulse; thus, the contribution of the calcium-induced release to the overall R_{rel} was smaller and hence the suppression of the peak.

The above line of reasoning is valid for strong injections, too, and thus the loss of the peak could be a consequence of complete preinactivation. The $[Ca^{2+}]$ in the myoplasm causing full inactivation, however, is estimated to be >1 μM (Simon, Klein, and Schneider, 1991), two orders of magnitude higher then that actually measured in case of the fiber shown in Fig. 2.

Noise in the R_{rel} Records after Injection

Records after injection were always more noisy than records before, and furthermore, traces from injections with lower affinity buffers tended to show more noise than those from injections using higher affinity buffers. Apart from the fact that the signal-to-noise ratio was smaller after injection than before, much of the noise arose from the different types of calculation used before and after injection.

The steps to obtain R_{rel} involve calculating calcium binding to sites (roughly equivalent to integrating the $[Ca^{2+}]$ transient) and then taking their derivative (see Eq. 4). This will result in noise in R_{rel} comparable to that in the calcium transient used in the calculation. Before injection the calculation of R_{rel} was based mainly on the APIII calcium transient, which had, assuming instantaneous equilibrium, the same noise as the optical detection system itself. Consequently, the noise in R_{rel} before injection was comparable to the noise of the absorbance signal. After a strong injection of fura-2 or BAPTA, $\Delta[Ca^{2+}]$ was calculated from [Ca-fura-2], which introduced a noise comparable to the derivative of the measured fluorescence into the calculated $[Ca^{2+}]$ (Eq. 2). Unlike fura-2 and BAPTA, in the case of F_2BAPTA and Br_2BAPTA the calculated calcium bound to the buffer was more noisy than the measured fluorescence, since the $k_{off,B}$ value used to calculate the binding was greater than the $k_{off,f}$ value used for calculating the calcium transient. This resulted in R_{rel} records with even more noise than the derivative of the measured fluorescence such that the lower the affinity of the buffer the greater the noise in the calculated R_{rel}.

Parameters of the "Intrinsic" Calcium Binding Sites

To calculate the removal parameters, the decay of the APIII calcium transients before injection was usually fit by adjusting the values of three of the parameters, $k_{off,Mg\text{-}parvalbumin}$, [parvalbumin], and PV_{max}. Using standard values (cf. Klein et al., 1990) for all the other parameters, decent fits could be obtained to the declining phase of the calcium transients before injection. This was, however, not the case for the slow decline of the calcium transient measured after injection, as shown in Fig. 10.

Alternative sets of removal parameter values were obtained by including the record from after injection in the fit and by changing all parameters stepwise for successive fits. The fitted parameters were the same as in the original calculation. Though this method resulted in greatly improved fits, even for records not included in the fit (see Fig. 10 *B*), the changes in parameter values obtained with different fibers were diverse.

In general, if the estimated SR calcium content, obtained from the depletion correction after a strong injection, was similar to that before injection, the original parameters were satisfactory after the injection, too. On the other hand, if the estimated content after injection exceeded that before injection, the new parameters tended to increase the calcium bound to the fast buffers, that is, to troponin C and/or the SR calcium pump. This increase, however, was achieved differently in different fibers. In some cases, like the fiber in Fig. 10, the sole, but large, increase in the concentration of troponin C gave the best result. In others, a smaller increase in the [troponin C] together with an increase in the affinity of troponin C for calcium was needed, and sometimes the affinity of the pump had to be increased as well. Since we could not come up with a general solution that could be applied to each and every fiber, and furthermore, the numbers obtained (e.g., [troponin C] = 880 μM in Fig. 10) were far from those measured biochemically, the original values for the removal parameters were used throughout for standard calculations of R_{rel}.

It is worth noting, however, that the above mentioned trend of increased calcium binding to fast buffers is probably correct and represents a true underestimation of the calcium bound to noninjected sites in the standard calculations. Whether this is due to an actual underestimation of the binding sites and/or their calcium affinity, or to an incorrect scaling of the APIII calcium transients (Maylie, Irving, Sizto, and Chandler, 1987) awaits further elucidation.

Time Course of the Number of Open Calcium Release Channels in the SR

To allow the comparison of the rate of release before and after injection, that is, when the calculation was based predominantly on calcium bound to the noninjected and injected sites, respectively, R_{rel} was corrected for depletion and normalized to the estimated SR calcium contents (R^*_{rel}/C_o). Apart from utilizing the fact that the SR content should not have changed during the injection, this normalization results in records that are proportional to the number of open channels, as shown below, under the constraints that all channels have the same conductance and the free [Ca^{2+}] in the SR is much greater than in the myoplasm.

Let $j(t)$ denote the flux of calcium through a single release channel from the SR

into the myoplasm at time t. According to Fick's first law:

$$j(t) = -D\partial C(x)/\partial x \tag{7}$$

where D is the diffusion coefficient and $\partial C(x)/\partial x$ is the concentration gradient of calcium. To convert the flux into the units of our measured value, R_{rel}, which is the rate of change in concentration, Eq. 7 should be multiplied by the cross-section of the channel (A) and divided by the total volume of the myoplasm (V_{myo}). Assuming that the concentration inside ($C_i(t)$) and outside ($C_o(t)$) the SR and the single channel conductance are the same for each and every channel, and that there are $N(t)$ channels open at time t, the total rate of release, $R_{rel}(t)$, can be written as

$$R_{rel}(t) = N(t)\cdot A/V_{myo}\cdot D\cdot[C_i(t) - C_o(t)]/l \tag{8}$$

where l denotes the length of a channel. Since R_{rel} is actually calculated from the bulk myoplasmic calcium transient, $C_o(t)$ and l in Eq. 8 should be understood as the myoplasmic $[Ca^{2+}]$ and an apparent diffusion length between the SR lumen and the myoplasmic space, respectively. Solving Eq. 8 for $N(t)$ using the fact that A, D, V_{myo}, and l are independent of time,

$$N(t) = k\cdot R_{rel}(t)/[C_i(t) - C_o(t)] \tag{9}$$

where k is a proportionality coefficient equal to $V_{myo} \cdot l/D/A$. Assuming that the calcium concentration in the SR is much greater than in the myoplasm, Eq. 9 becomes

$$N(t) = k\cdot R_{rel}(t)/C_i(t) \tag{10}$$

$C_i(t)$ can be calculated as the $[Ca^{2+}]$ in the SR at time 0, i.e., $C \cdot (0)$, minus that released up to time t. Let V_{SR} denote the volume of the SR, whereas E_{myo} and E_{SR} denote the volume expansion (for definition see Kovács et al., 1983) due to calcium binding proteins within the myoplasm and SR lumen, respectively:

$$C_i(t) = [C_0 - I(t)]/[(V_{myo}\cdot E_{myo})/(V_{SR}\cdot E_{SR})] \tag{11}$$

where C_0 and $I(t)$ are the calcium content of the SR before a stimulus and the running integral of R_{rel} (above). Using Eq. 11 for $C_i(t)$ and including the divider from Eq. 11 into k, Eq. 10 transforms to

$$N(t) = k^*\cdot R_{rel}(t)/[C_0 - I(t)] \tag{12}$$

The right-hand side of Eq. 12, apart from the proportionality coefficient, is R_{rel} corrected for depletion of calcium from the SR and normalized to SR content, which is thus proportional to the number of open calcium release channels in the SR membrane.

In the above calculation the flux through the individual channels was assumed to be independent of the concentration of all ions present (Eq. 7). This might not be the case since saturation of the channel at millimolar $[Ca^{2+}]$ can occur (for review see Williams, 1992), but as long as the channels behave, statistically, the same the conclusion that R^*_{rel}/C_o is proportional to $N(t)$ is still valid.

We are greatly indebted to Dr. J. P. Y. Kao for advice concerning the use of calcium buffers and for custom synthesis of the anisidine used in these experiments. We thank Gerard Vaio and Alex

Bustamante for technical assistance, Dr. Michael G. Klein for help with various aspects of data acquisition and analysis, Mária Csernoch for help with figure preparations, Gabe Sinclair and Walt Knapick for constructing mechanical and optical apparatus, Jeff Michael and Chuck Leffingwell for electronics support, and Dr. Stephen Baylor for sending us preliminary versions of a recent paper from his laboratory (Hollingworth et al., 1992).

This work was supported by research grants from the NIH (R01-NS-23346) and the Muscular Dystrophy Association. Dr. Csernoch was the recipient of an MDA postdoctoral fellowship. Dr. Jacquemond was partially supported by the Melzer Foundation.

Original version received 15 July 1992 and accepted version received 6 October 1992.

REFERENCES

Armstrong, C. M., F. Bezanilla, and P. Horowicz. 1972. Twitches in the presence of ethylene glycol *bis*(β-aminoethyl ether)-N,N,N',N'-tetraacetic acid. *Biochimica et Biophysica Acta.* 267:605–608.

Baylor, S. M., and S. Hollingworth. 1988. Fura-2 calcium transients in frog skeletal muscle fibres. *Journal of Physiology.* 403:151–192.

Beuckelmann, D. J., and W. G. Wier. 1988. Mechanism of release of calcium from sarcoplasmic reticulum of guinea-pig cardiac cells. *Journal of Physiology.* 405:233–255.

Block, B. A., T. Imagawa, K. P. Campbell, and C. Franzini-Armstrong. 1988. Structural evidence for direct interaction between the molecular components of the transverse tubule/sarcoplasmic reticulum junction in skeletal muscle. *Journal of Cell Biology.* 107:2587–2600.

Brum, G., E. Stefani, and E. Ríos. 1987. Simultaneous measurement of Ca^{2+} current and intracellular Ca^{2+} concentrations in single skeletal muscle fibres of the frog. *Canadian Journal of Physiology and Pharmacology.* 65:681–685.

Caputo, C. 1972. The time course of potassium contractures of single muscle fibres. *Journal of Physiology.* 223:483–505.

Chandler, W. K., R. F. Rakowski, and M. F. Schneider. 1976. Effects of glycerol treatment and maintained depolarization on charge movement in skeletal muscle. *Journal of Physiology.* 254:285–316.

Close, R. I. 1981. Activation delays in frog twitch muscle fibres. *Journal of Physiology.* 313:81–100.

Crank, J. 1975. The Mathematics of Diffusion. Oxford University Press, New York. 11–12.

Csernoch, L., V. Jacquemond, J. P. Y. Kao, and M. F. Schneider. 1992. The effect of BAPTA type calcium buffers on the calcium release in frog skeletal muscle fibers. *Biophysical Journal.* 61:23*a*. (Abstr.)

Endo, M. 1985. Calcium release from the sarcoplasmic reticulum. *Current Topics in Membranes and Transport.* 25:181–229.

Endo, M., M. Tanaka, and Y. Ogawa. 1970. Calcium-induced release of calcium from the sarcoplasmic reticulum of skinned skeletal muscle fibers. *Nature.* 228:34–36.

Fabiato, A. 1984. Dependence of the calcium-induced release from the sarcoplasmic reticulum of skinned skeletal muscle fibers from the frog semitendinosus on the rate of change of free Ca^{2+} at the outer surface of the of the sarcoplasmic reticulum. *Journal of Physiology.* 353:56a. (Abstr.)

Fleischer, S., E. M. Ogunbunmi, M. C. Dixon, and E. A. M. Fleer. 1985. Localization of the Ca^{2+} release channels with ryanodine in junctional terminal cisternae of sarcoplasmic reticulum of fast skeletal muscle. *Proceedings of the National Academy of Sciences, USA.* 87:7256–7259.

Ford, L. E., and R. J. Podolsky. 1970. Regenerative calcium release within muscle cells. *Science.* 167:58–59.

Frank, G. B. 1958. Inward movement of calcium as a link between electrical and mechanical events in contraction. *Nature.* 151:518–538.

Grynkiewicz, G., M. Poenie, and R. Y. Tsien. 1985. A new generation of Ca^{2+} indicators with greatly improved fluorescence properties. *The Journal of Biological Chemistry.* 260:3440–3450.

Harrison, S. M., and D. M. Bers. 1987. The effect of temperature and ionic strength on the apparent Ca-affinity of EGTA and the analogous Ca-chelators BAPTA and dibromo-BAPTA. *Biochimica et Biophysica Acta.* 925:133–143.

Haugland, R. P. 1989. Handbook of Fluorescent Probes and Research Chemicals. Molecular Probes, Inc., Eugene, OR. 78–85.

Hollingworth, S., A. B. Harkins, N. Kurebayashi, M. Konishi, and S. M. Baylor. 1992. Excitation-contraction coupling in intact frog skeletal muscle fibers injected with molar concentrations of fura-2. *Biophysical Journal.* 63:224–234.

Imagawa, T., J. S. Smith, R. Coronado, and K. P. Campbell. 1987. Purified ryanodine receptor from skeletal muscle sarcoplasmic reticulum is the Ca^{2+}-permeable pore of the calcium release channel. *Journal of Biological Chemistry.* 262:16636–16643.

Irving, M., J. Maylie, N. L. Sizto, and W. K. Chandler. 1989. Simultaneous monitoring of changes in magnesium and calcium concentrations in frog cut twitch fibers containing antipyrylazo III. *Journal of General Physiology.* 93:585–608.

Jacquemond, V., L. Csernoch, M. G. Klein, and M. F. Schneider. 1991*a*. Voltage-gated and calcium-gated calcium release during depolarization of skeletal muscle fibers. *Biophysical Journal.* 60:867–873.

Jacquemond, V., M. G. Klein, and M. F. Schneider. 1990. Intracellular calcium and magnesium movements following calcium release in frog skeletal muscle. *Biophysical Journal.* 57:342*a*. (Abstr.)

Jacquemond, V., M. G. Klein, and M. F. Schneider. 1991*b*. Early and late antipyrylazo III signals consistent with decreased myoplasmic $[Mg^{2+}]$ during and after depolarization of frog skeletal muscle fibers. *Biophysical Journal.* 59:242*a*. (Abstr.)

Jacquemond, V., and M. F. Schneider. 1992. Effects of low myoplasmic Mg^{2+} on calcium binding by parvalbumin and calcium uptake by sarcoplasmic reticulum in frog skeletal muscle. *Journal of General Physiology.* 100:1–21.

Kao, J. P. Y., and R. Tsien. 1988. Ca^{2+} binding kinetics of Fura-2 and Azo-1 from temperature-jump relaxation measurements. *Biophysical Journal.* 54:635–639.

Klein, M. G., B. J. Simon, and M. F. Schneider. 1990. Effects of caffeine on calcium release from the sarcoplasmic reticulum in frog skeletal muscle fibres. *Journal of Physiology.* 425:599–626.

Klein, M. G., B. J. Simon, G. Szücs, and M. F. Schneider. 1988. Simultaneous recording of calcium transients in skeletal muscle using high and low affinity calcium indicators. *Biophysical Journal.* 55:971–988.

Konishi, M., A. Olson, S. Hollingworth, and S. M. Baylor. 1988. Myoplasmic binding of Fura-2 investigated by steady-state fluorescence and absorbance measurements. *Biophysical Journal.* 54: 1089–1104.

Kovács, L., E. Ríos, and M. F. Schneider. 1983. Measurement and modification of free calcium transients in frog skeletal muscle fibres by a metallochromic indicator dye. *Journal of Physiology.* 343:161–196.

London, B., and J. W. Krueger. 1986. Contraction in voltage-clamped, internally perfused single heart cells. *Journal of General Physiology.* 88:475–505.

Lüttgau, H. C. 1963. The action of calcium ions on potassium contractures of single muscle fibres. *Journal of Physiology.* 168:679–697.

Lüttgau, H. C., and W. Spiecker. 1979. The effects of calcium deprivation upon mechanical and electrophysiological parameters in skeletal muscle fibres of the frog. *Journal of Physiology.* 296:411–429.

Maylie, J., M. Irving, N. L. Sizto, and W. K. Chandler. 1987. Calcium signals recorded from cut frog twitch fibers containing antipyrylazo III. *Journal of General Physiology.* 89:83–143.

Meissner, G., E. Darling, and J. Eveleth. 1986. Kinetics of rapid Ca2+ release by sarcoplasmic reticulum. Effects of Ca^{2+}, Mg^{2+}, and adenine nucleotides. *Biochemistry.* 25:236–244.

Melzer, W., E. Ríos, and M. F. Schneider. 1987. A general procedure for determining calcium release from the sarcoplasmic reticulum in skeletal muscle fibers. *Biophysical Journal.* 51:849–863.

Pethig, R., M. Kuhn, R. Payne, E. Adler, T.-H. Chen, and L. F. Jaffe. 1989. On the dissociation constants of BAPTA-type calcium buffers. *Cell Calcium.* 10:491–498.

Pizarro, G., L. Csernoch, I. Uribe, and E. Ríos. 1992. Differential effects of tetracaine on two kinetic components of calcium release in frog skeletal muscle fibres. *Journal of Physiology.* 457:525–538.

Ríos, E., and G. Brum. 1987. Involvement of dihydropyridine receptors in excitation-contraction coupling in skeletal muscle. *Nature.* 325:717–720.

Ríos, E., M. Karhanek, A. González, and J. Ma. 1992*a*. An allosteric model of transmission in E-C coupling. *Biophysical Journal.* 61:131*a*. (Abstr.)

Ríos, E., and G. Pizarro. 1988. Voltage sensors and calcium channels of excitation-contraction coupling. *News in Physiological Sciences.* 3:223–228.

Ríos, E., and G. Pizarro. 1991. Voltage sensor of excitation-contraction coupling in skeletal muscle. *Physiological Reviews.* 71:849–908.

Ríos, E., G. Pizarro, and E. Stefani. 1992*b*. Charge movement and the nature of signal transduction in skeletal muscle excitation-contraction coupling. *Annual Reviews of Physiology.* 54:109–133.

Schneider, M. F., and W. K. Chandler. 1973. Voltage dependent charge movement in skeletal muscle. *Nature.* 242:244–246.

Schneider, M. F., and B. J. Simon. 1988. Inactivation of calcium release from the sarcoplasmic reticulum in frog skeletal muscle. *Journal of Physiology.* 405:727–745.

Schneider, M. F., B. J. Simon, and M. G. Klein. 1989. Decline of calcium release from the sarcoplasmic reticulum in skeletal muscle cells due to inactivation and calcium depletion. *In* Physiology and Pharmacology of Transmembrane Signalling. T. Segawa, M. Endo, M. Ui, and K. Kurihara, editors. Elsevier Science Publishers, Amsterdam. 253–260.

Schneider, M. F., B. J. Simon, and G. Szücs. 1987. Depletion of calcium from the sarcoplasmic reticulum during calcium release in frog skeletal muscle. *Journal of Physiology.* 392:167–192.

Simon, B. J., and D. A. Hill. 1992. Charge movement and SR calcium release in frog skeletal muscle can be related by a Hodgkin-Huxley model with four gating particles. *Biophysical Journal.* 61:1109–1116.

Simon, B. J., M. G. Klein, and M. F. Schneider. 1991. Calcium dependence of inactivation of calcium release from the sarcoplasmic reticulum in skeletal fibers. *Journal of General Physiology.* 97:437–471.

Simon, B. J., and M. F. Schneider. 1988. Time course of activation of calcium release from sarcoplasmic reticulum in skeletal muscle. *Biophysical Journal.* 54:1159–1163.

Smith, G. A., R. T. Hesketh, J. C. Metcalfe, J. Feeney, and P. G. Morris. 1983. *Proceedings of the National Academy of Sciences, USA.* 80:7178–7182.

Smith, J. S., R. Coronado, and G. Meissner. 1986. Single channel measurements of the calcium release channel from skeletal muscle sarcoplasmic reticulum. Activation by Ca^{2+} and ATP and modulation by Mg^{2+}. *Journal of General Physiology.* 88:573–588.

Tanabe, T., H. Takeshima, A. Mikami, H. Matsuo, T. Hirose, and S. Numa. 1987. Primary structure of the receptor for calcium channel blockers from skeletal muscle. *Nature.* 328:313–318.

Tsien, R. Y. 1980. New calcium indicators and buffers with high selectivity against magnesium and protons: design, synthesis, and properties of prototype structures. *Biochemistry.* 19:2396–2404.

Williams, A. J. 1992. Ion conduction and discrimination in the sarcoplasmic reticulum ryanodine receptor/calcium-release channel. *Journal of Muscle Research and Cell Motility.* 13:7–26.

Xu, L., R. V. Jones, and G. Meissner. 1990. Tetracaine inhibition of the Ca release channel from skeletal sarcoplasmic reticulum. *Biophysical Journal.* 57:170*a*. (Abstr.)